UNITED STATES
DEPARTMENT OF THE INTERIOR
GEOLOGICAL SURVEY

Ages of flow units in the far eastern lunar maria based on crater density

by

Joseph M. Boyce
U. S. Geological Survey, Flagstaff, Arizona

This report is preliminary and has not been edited or reviewed for conformity with U.S. Geological Survey standards and nomenclature.

Prepared by the Geological Survey for the National Aeronautics and Space Administration

UNITED STATES
DEPARTMENT OF THE INTERIOR
GEOLOGICAL SURVEY

Ages of flow units in the far eastern lunar maria based on crater density

by

Joseph M. Boyce
U. S. Geological Survey, Flagstaff, Arizona

Open-file Report 78-879
1978

This report is preliminary and has not been edited or reviewed for conformity with U. S. Geological Survey standards and nomenclature.

Table of Contents

Illustrations

Abstract

The distribution of major geologic units of uniform relative age exposed in the far eastern maria (i.e., Mare Marginis, Mare Smythii, and Mare Crisium) and Mare Humorum was compiled in map form on the basis of a crater density mapping technique. Correlation of crater densities and radiometric ages of Apollo landing sites provide estimates of the absolute age for the units. Results indicate that the far eastern maria were emplaced over a period of approximately 1.25 b.y., from about 3.75 b.y. to 2.5 b.y. before present. Extensive young mare units ($\sim 2.5 \pm 0.5$ b.y.) occur in all three large far eastern maria. Major old units ($\sim 3.65 \pm 0.05$ b.y.) occur in central Mare Crisium and eastern Mare Marginis. Correlation of the age data and remote sensing data suggests that: (1) both young and old units have relatively high Mg/Al ratios and are relatively rich in Fe and Ti, whereas intermediate age units have lower Mg/Al ratios and less Fe and Ti. A similar relationship previously noted for other maria suggests that this applied throughout the lunar maria; (2) older units generally have higher remnant magnetism than younger units - a relationship also previously noted for other lunar maria and attributed to a steady decline of a primodial lunar magnetic field, and (3) all age units in the eastern maria have relatively low natural radioactivity or abundances of Th, K, and U compared to the western maria (particularly in the Mare Imbrium area). The presence of young lava flows in both the eastern and western maria suggests that the relative abundance of these radioactive elements has played only a minor role in controlling the duration and location of mare volcanism.

The crater-density relative age data presented here correlate in a linear fashion with crater-morphology relative age data. A combination of these data provides a nearly complete map of the distribution of units of uniform relative age of the lunar maria and shows that, as previously suggested, the older units (> 3.5 b.y. old) are generally located along the basin edges and the younger units (< 3.5 b.y. old) are generally in the basin centers. However, this map also shows that the vents for the flows of the young units must be located on the edges of the basins. These observations support tectonic models of basin subsidence caused by isostatic adjustment to the weight of the lava and to subsurface evacuation and subsequent collapse as the lavas were erupted.

Introduction

Relative age studies based on crater density and crater morphology have provided valuable information about the evolution and geologic history of the Moon. In most studies investigators determine the size-frequency distribution for small areas (for example see: Baldwin, 1969; Morris and Shoemaker, 1969; Hartmann, 1970; Greeley and Gault, 1970; Young, 1975; Neukum and others, 1975). These data are compared to size-frequency distributions determined for other areas to derive relative chronologies. Techniques to determine relative ages based on morphology of small (∿ 10 m-1 km) bowl-shaped craters (Soderblom and Lebofsky, 1972; Boyce and Dial, 1975) have been developed that provide a rapid and consistent method for obtaining relative age data. A nearly complete map of the distribution of major age units in the lunar nearside maria was produced by these techniques (Boyce, 1976). However, because of limitations of the technique and of poor quality photographs, the map excluded Mare Crisium, Mare Marginis, and Mare Smythii. A refined crater density mapping technique (Boyce and Johnson, 1977) was developed to map the distribution of major age units in Mare Crisium. This technique was applied to photographs of Mare Marginis and Mare Smythii. The technique has also been applied to photographs of Mare Humorum in order to compare relative ages from crater density mapping with those obtained from crater morphology studies.

The new crater density data presented here were combined with the crater density data of Boyce and Johnson (1977) to produce a complete map of the distribution of major age units in the lunar far eastern nearside maria. The crater density data can also be correlated directly with the crater morphology data of Boyce (1976) which cover most of the other lunar nearside maria.

Technique

Lunar Orbiter IV high-resolution photographs were used for counting craters in all sample areas except northern Mare Crisium, where Apollo metric photographs were used, and eastern Mare Smythii, where Lunar Orbiter I high-resolution photographs were used. All obvious secondary craters, rimless or endogenic craters and partially buried pre-mare craters > 900 m in diameter were mapped and excluded from the counts to ensure that only the population representing the average production function for craters larger than a particular diameter was included. The individual mare were subdivided into rectangular sample grids of from 153 km^2 to 256 km^2. The grid cell size was adjusted to individual mare size (small mare had smaller cells and large mare had larger cells) to increase the number of data points in the small mare and reduce data collection time for large mare. Craters over 900 m in diameter were counted in each cell, and that number is used as a measure of relative age of the cell. These data are listed in appendix 1-4. This size range was chosen because it includes craters that are small and numerous enough to provide adequate statistics for each area and large enough readily to separate primary from secondary or endogenic craters.

The crater density for each grid cell was digitized and transformed into an image array of real floating point numbers in a simple cylindrical projection with each image array element covering 0.25 degrees square (Eliason and Soderblom, 1977). The data were interpolated by spatial filtering into a continuous image and transformed into Mercator projection. The filter interpolates by averaging the points within a square neighborhood:

$$b_{ij} = \frac{\sum_{m=i-k}^{i+k} \sum_{n=j-k}^{j+k} \delta_{mn} B_{mn}}{\sum_{m=i-k}^{i+k} \sum_{n=j-k}^{j+k} \delta_{mn}},$$

where b_{ij} are the interpolated values, B_{mn} are the discrete points of raw data to be averaged, which are sparsely located throughout the array, and k is the size of the neighborhood or smoothing area each of which are 0.25 degrees square. The delta function, δ_{mn}, allows the discrimination between discrete points and non-data points in the image array. Although the technique increases the statistical weight of the data, the smoothing decreases the resolution of data by a factor of 2k+1.

Figure 1 is a histogram of the data after smoothing using a moving average based on a 9 x 9 neighborhood. Figure 2 shows the map distribution of the smoothed data. This size filter provides good resolution but at a cost of statistical confidence. Figure 3 is a histogram of the data after smoothing using a 21 x 21 neighborhood, and figure 4 shows the map distribution of these smoothed data. This size neighborhood provides a balance between adequate statistical confidence (a 21 x 21 neighborhood provides a factor of seventeen times the number of crater, 2 to 35, than does the 9 x 9 neighborhood for the most sparsely cratered area) and resolution. We therefore have used this as the standard smoothing for our data. A major drawback to any crater counting technique is the averaging of areally small units. The smoothing technique tends to amplify this problem. Therefore, only major units can be confidently identified.

Figure 3 shows smoothed crater density data divided into four major modes. The modes are based on standard crater count data for individual age units. The data were further processed by imaging gray levels to the

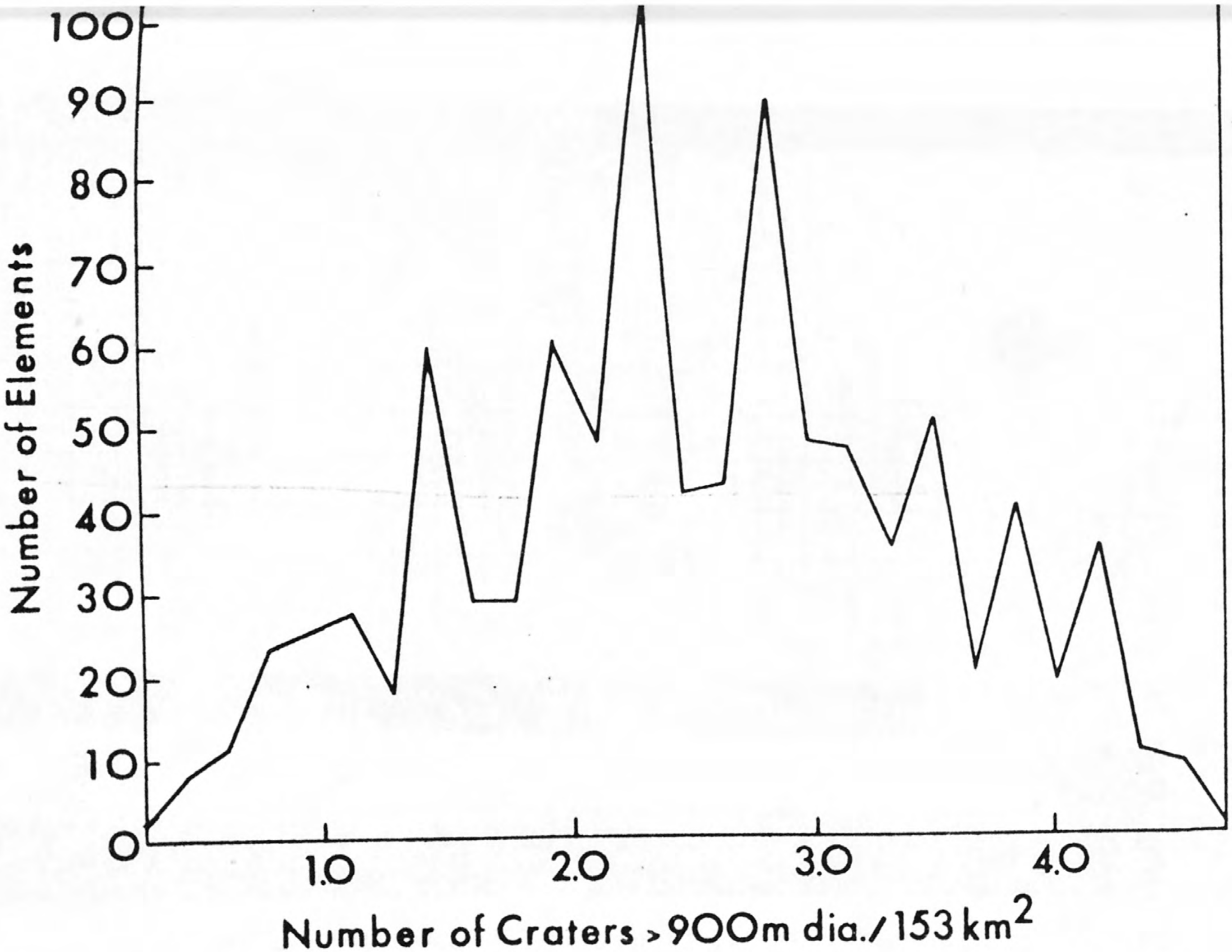

Figure 1. Histogram of crater densities after computer smoothing using a 9 x 9 neighborhood for Mare Crisium, Mare Marginis, Mare Smythii, and Mare Humorum.

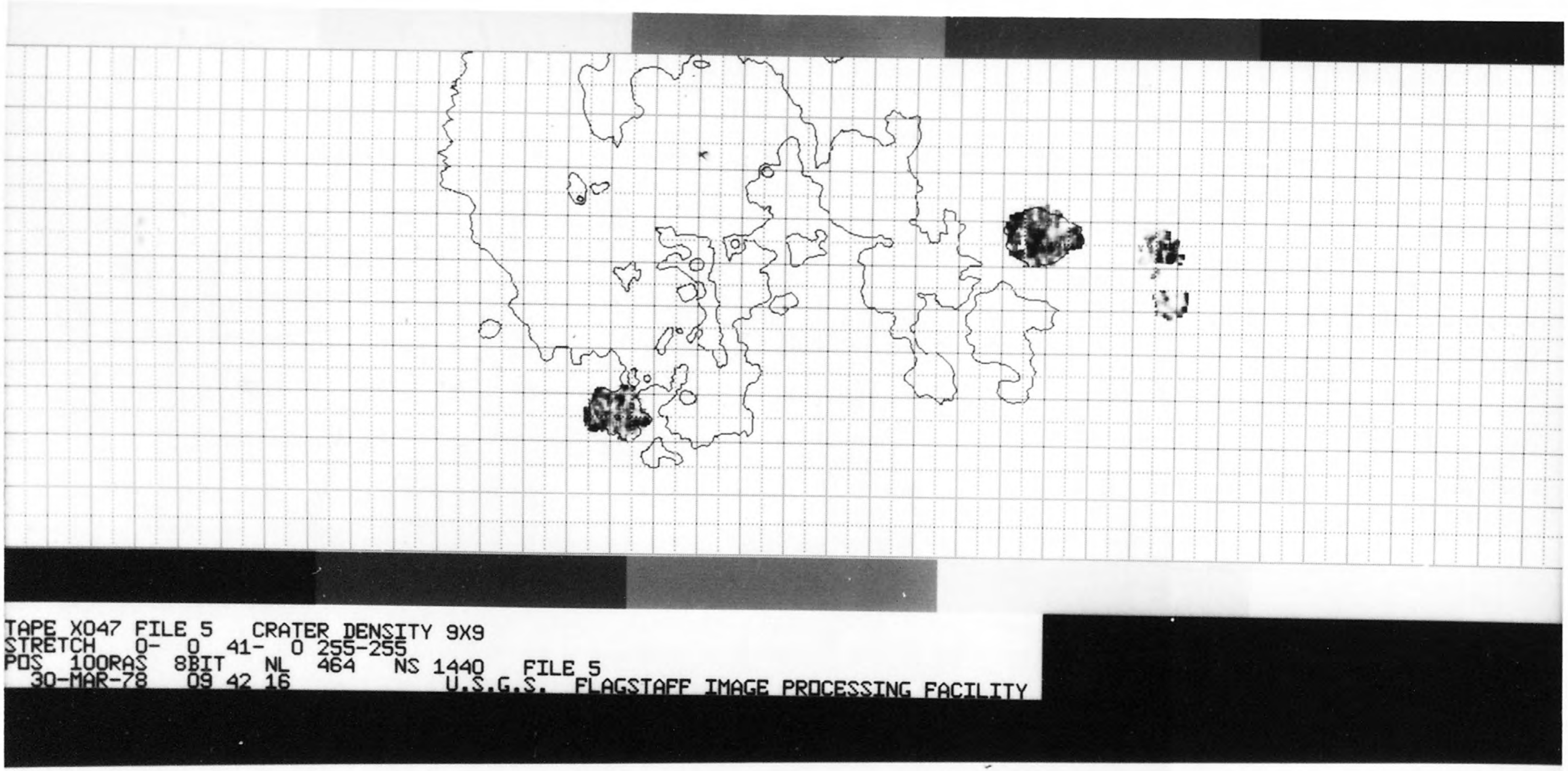

Figure 2. Distribution of crater densities in Mare Crisium, Mare Marginis, Mare Smythii, and Mare Humorum. The raw data have been smoothed using a 9 x 9 neighborhood. The gray level corresponds to crater density (darkest equals most heavily cratered).

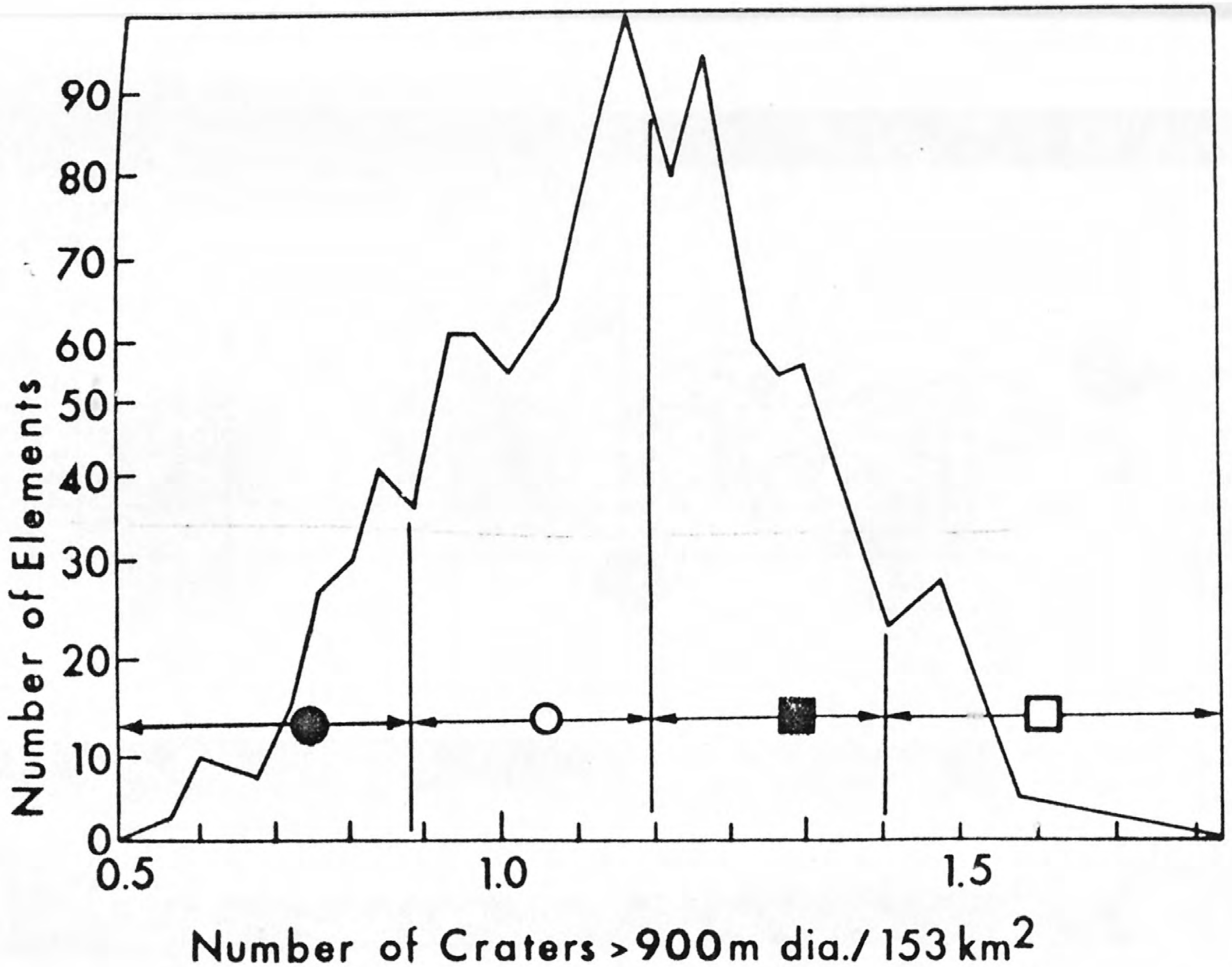

Figure 3. Histogram of crater densities after computer smoothing using a 21 x 21 neighborhood for Mare Crisium, Mare Marginis, Mare Smythii, and Mare Humorum. Solid circles = unit IV (the youngest unit); open circle = unit III (Apollo 12 age); solid square = unit II (Apollo 15 age); and open square = unit I (Apollo 11 age).

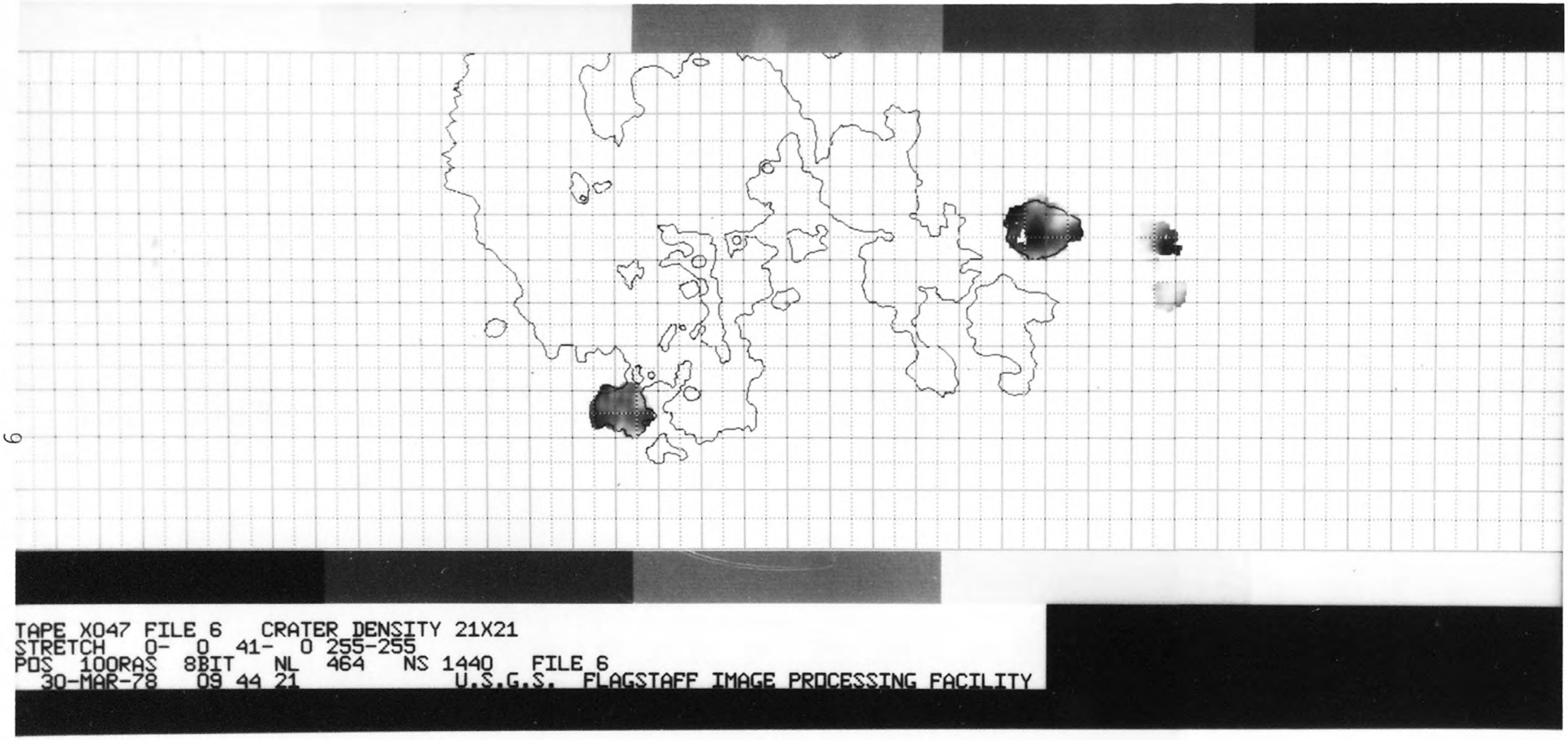

Figure 4. Distribution of crater densities in Mare Crisium, Mare Marginis, Mare Smythii, and Mare Humorum. The data have been smoothed using a 21 x 21 neighborhood. The gray levels corresponds to crater density (darkest equals most heavily cratered).

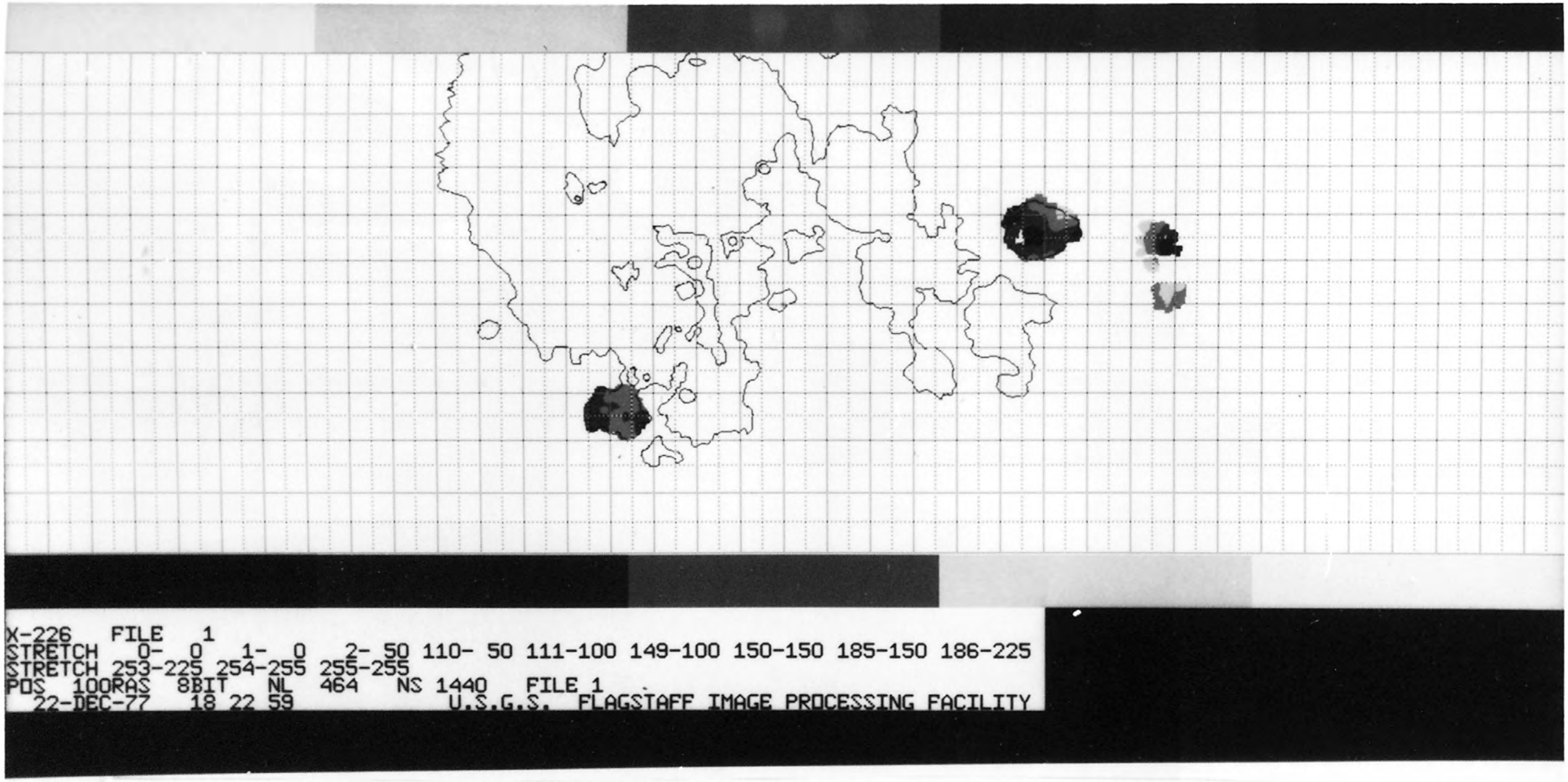

Figure 5. Distribution of major relative age (crater density) units in Mare Crisium, Mare Marginis, Mare Smythii, and Mare Humorum. The four major age units are shown as different levels of gray (darkest equals oldest).

crater density range of each of the four modes. This technique was previously applied by Boyce and Johnson (1977) for the three major age units in Mare Crisium using a 17 x 17 neighborhood for smoothing. Figure 5 shows the resulting map with the decreasing gray levels corresponding to decreasing crater density (the oldest unit is the darkest). Smoothing of boundaries between units of widely differing age produces artificial intermediate age units along the boundary. The effect appears in northeastern Mare Crisium and west-central Mare Marginis.

Results and Discussions

The distribution of relative age units in the eastern maria and Mare Humorum shown in figure 5 indicates that the oldest unit (unit I) is found in the northwest, central, and eastern parts of Mare Crisium, the eastern part of Mare Marginis, and the southwest part of Mare Humorum. Flows of the next oldest unit (unit II) are located in the north-central, southwest, and southeast parts of Mare Crisium, and the west half and the southeastern part of Mare Humorum. The next youngest unit (unit III) is found in the central part of Mare Marginis, along the southern, western and eastern edges of Mare Smythii, and the east half of Mare Humorum. The next youngest unit (unit IV) is found in the north and south of Mare Crisium, the western part of Mare Marginis, and the central and northern parts of Mare Smythii.

The absolute ages of the relative age units can be estimated by comparing crater densities on areas with known absolute ages (from Apollo landing sites) with the crater densities of the units. The age (both relative and absolute) of each units has been estimated previously (Neukum and others, 1975; Boyce and Johnson, 1977; Boyce and others, 1977) with the exception of unit III. Since the density of craters on unit III is intermediate between unit IV (the youngest unit) and unit II (Apollo 15 age) it was expected to be approximately Apollo 12 site in age. To verify this, the average crater density of unit III (taken from the histograms in Figure 3) was compared with the crater size-frequency data for the older unit at the Apollo 12 site (as described by Soderblom and Lebofsky, 1972) which is shown in Figure 6. As previously done by Boyce and others (1977) and Boyce and Johnson (1977), the absolute age ranges of the four subdivisions can be estimated using the crater density data of Morris and Shoemaker (1969) for Apollo 11 site, Lucchitta and Sanchez (1975) for Apollo 17 site, Boyce (1976) for North Ray Crater and, Boyce and others (1977) for Apollo 15 site, and the new crater density data presented here for Apollo 12 site, calibrated with sample ages for the landing sites (Papanastassiou and Wasserburg, 1971; Wasserburg and Papanastassiou, 1971; Evensen and others, 1973; Drozd and others, 1974; Marti and others, 1973). This relationship is illustrated in Figure 7 and shows the following: (1) unit I = 3.65 $\pm$ 0.05 b.y.; (2) unit II = 3.5 $\pm$ 0.1 b.y.; (3) unit III = 3.2 $\pm$ 0.2 b.y.; and (4) unit IV = 2.5 $\pm$ 0.5 b.y. The estimated error limits are based on the values of relative age unit boundaries plotted on the calibrated flux curve shown in Figure 7. An older units about 3.75 $\pm$ 0.05 b.y. (Boyce and others, 1977) is below the resolution used in this study and is not discussed here.

These absolute ages provide a means to readily compare the age data based on crater density presented here with ages derived from crater morphology by Boyce (1976). The fact that both relative age dating

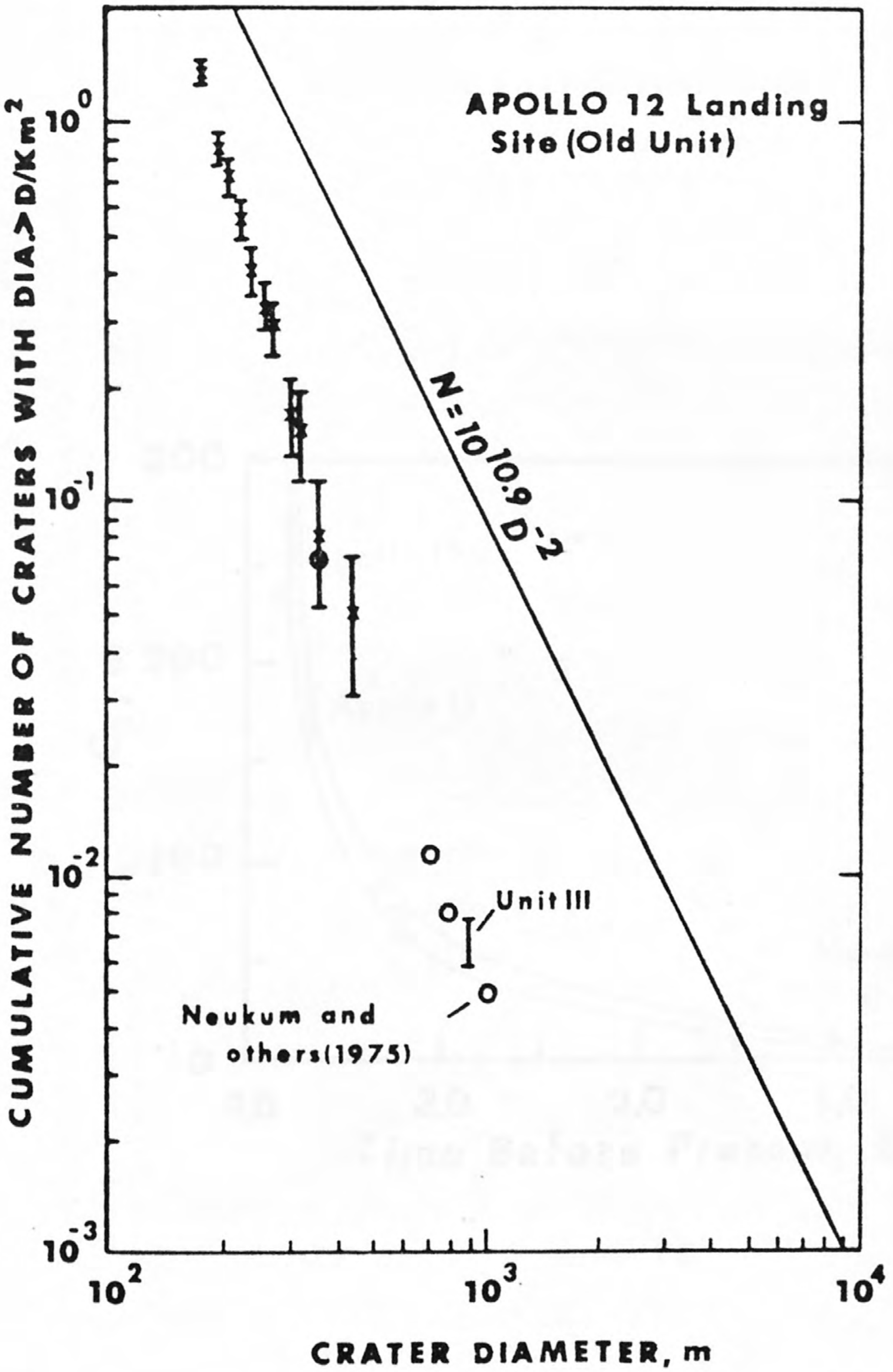

Figure 6. Comparison of the cumulative size frequency of craters formed in the old unit at the Apollo 12 site and the average number of craters larger than 900 m diameter formed on Unit III. Error bars are based on an estimate of one standard deviation ($\pm\sqrt{N}$). The open circles are data from Neukum and others (1975).

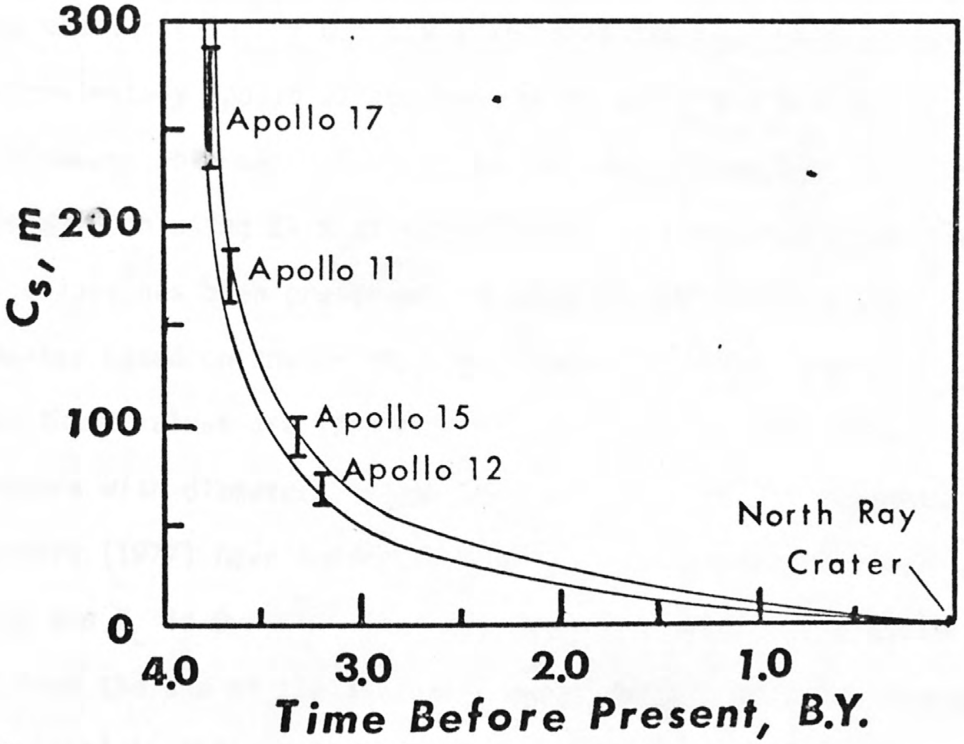

Figure 7. Comparison of relative age (C_s) of Apollo landing sites and North Ray Crater and radiometric ages.

techniques give equivalent absolute ages can be verified by comparing the distribution of age units in Mare Humorum that have been analyzed by using both techniques. The distribution of age units in Mare Humorum based on crater density is shown in Figure 8, and the distribution of age units in Mare Humorum based on small crater morphology (Boyce, 1976) is shown in Figure 9. Both maps of Mare Humorum show that the west half and south-east edge of Mare Humorum contain flows of approximately Apollo 15 - Luna 16 age basalts ($\sim 3.5 \pm 0.1$ b.y.) and that the east half contains flows of approximately Apollo 12 age basalts ($\sim 3.2 \pm 0.2$ b.y.).

Although both sets of data (density and morphology) have been computer smoothed (both using 21 x 21 neighborhoods), the proportionality between their values has been preserved. A plot of the values of the major unit boundaries based on crater density (Figure 10) shows that within error limits these values are linearly proportional (D_L = 211 times the number of craters with diameters larger than 900 m/153 km^2). However, Neukum and others (1977) have indicated that the relationship between crater density and D_L is $D \simeq N^{0.6}$ for craters on the maria. The difference may arise from the use of statistically small amounts of data (fourteen data points) in this earlier study to derive the relationship. In contrast, the data presented here are based on several thousand crater density determinations (encompassing four entire maria) and over a thousand crater morphology age determinations.

Therefore, the distribtuion of major age units in the far eastern maria determined here on the basis of crater density can be compared and correlated directly with the major age units determined by Soderblom and Lebofsky (1972) and Boyce (1976) using small crater morphology techniques.

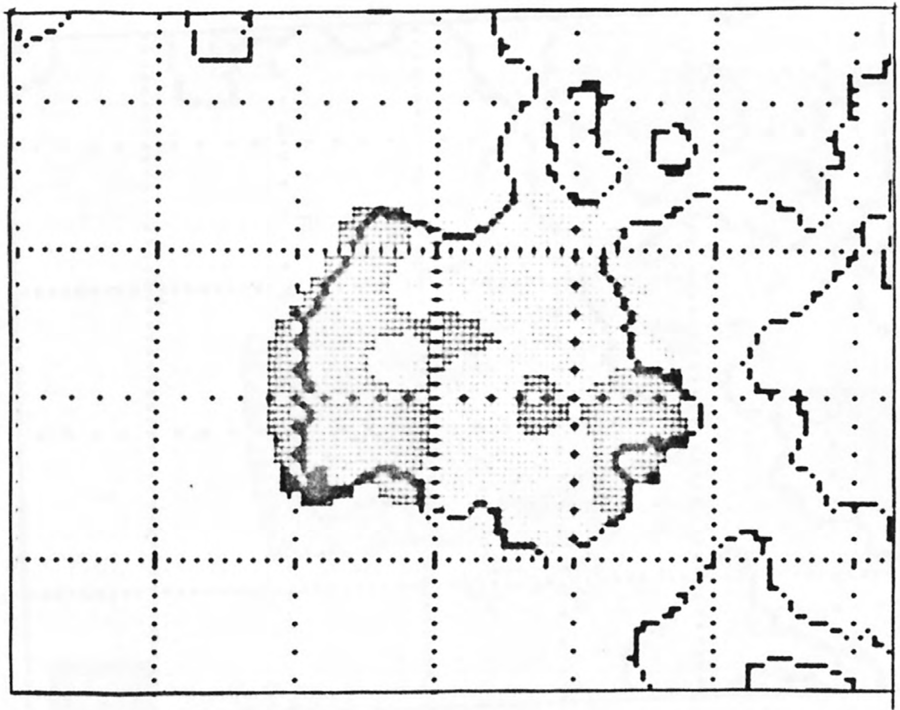

Figure 8. Distribution of relative age units in Mare Humorum based on crater density.

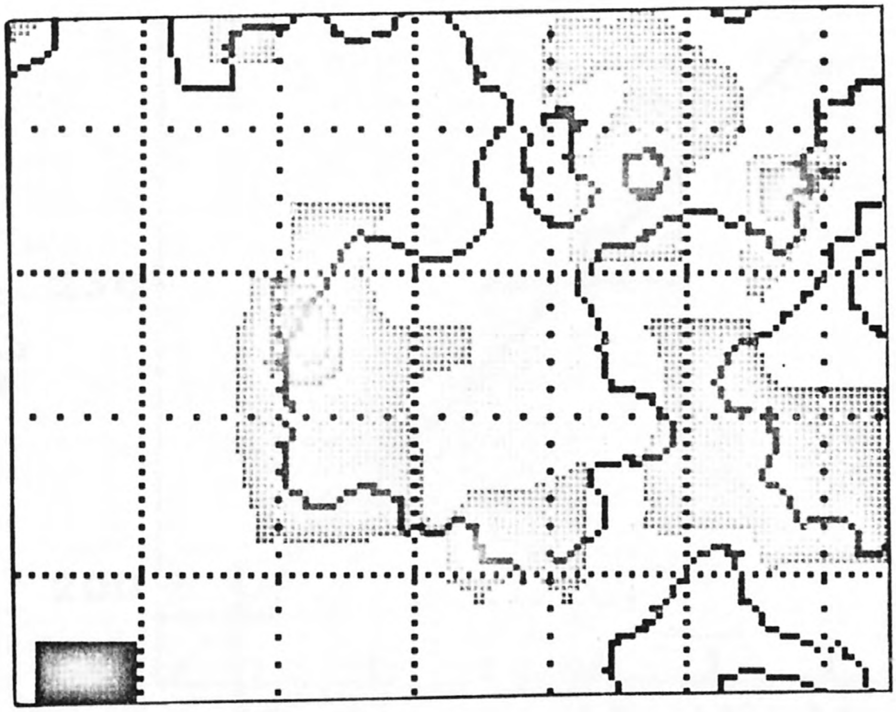

Figure 9. Distribution of relative age units in Mare Humorum based on the morphology of small craters.

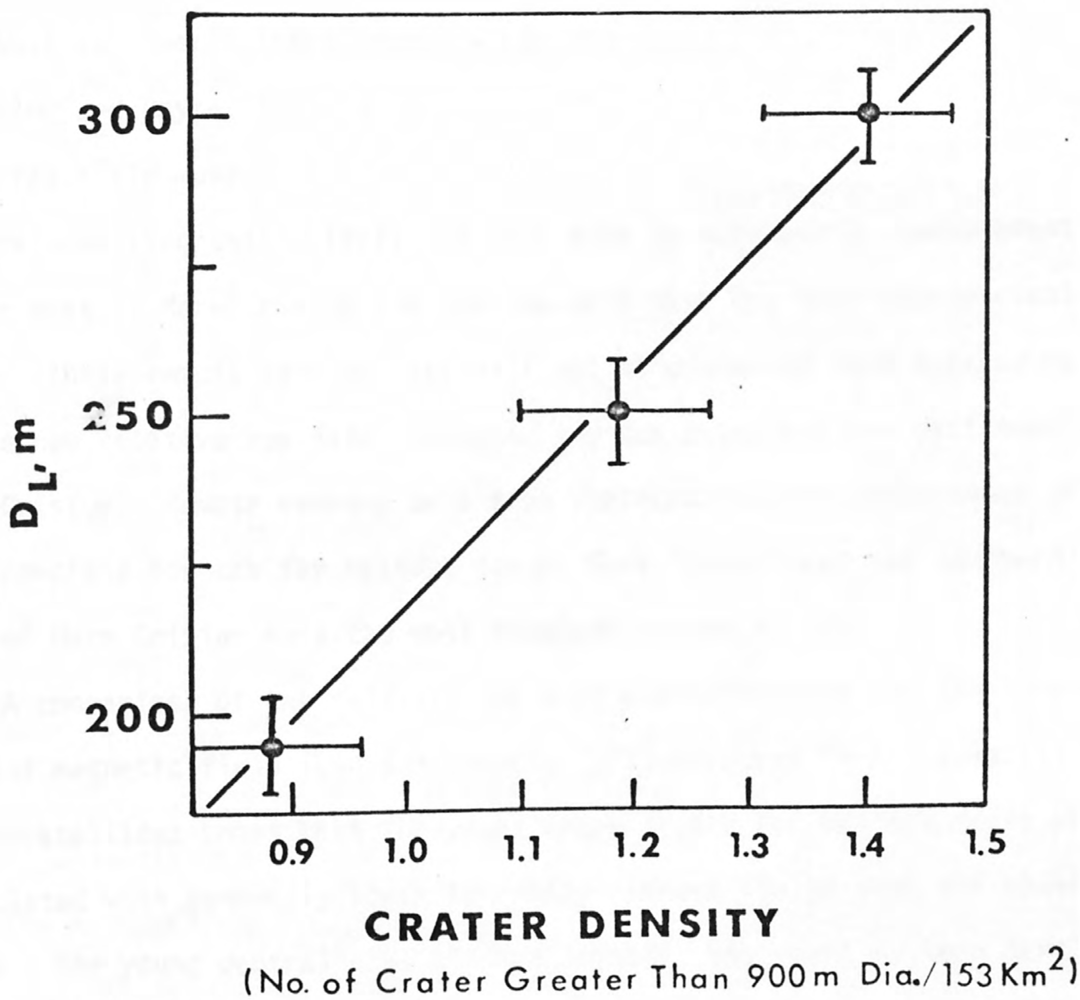

Figure 10. Relationship of major mare age unit boundary values based on modes in the smoothed histograms of the crater density data presented here and on crater morphology data (Boyce, 1976). Error bars are based on an estimate of one standard deviation ($\pm \sqrt{N}$).

The distribution of age units shown in figure 5 can be correlated with remote sensing data to provide information about the geologic evolution of the far eastern maria. Earth-based techniques such as measurement of visual and near infrared spectra (Whitaker, 1972; McCord, 1968; Soderblom and Boyce, 1976; Johnson and others, 1977; Pieters and others, 1978) radar (Thompson, 1970; Zisk and others, 1973) and infrared eclipse temperatures (Shorthill, 1973) are only able to make useful measurements as far east as Mare Crisium and for the most part are only poorly resolved there. These remote sensing data will not be discussed here because most of the new relative age data presented are for areas farther east than Mare Crisium. Remote sensing data from spacecraft-borne instruments are more complete for the far eastern maria; Mare Smythii and the southern part of Mare Crisium have the most complete coverage.

A comparison of the relative age data presented here and the lunar remnant magnetic field (Lin and others, 1977) measured from the Apollo 15 and 16 subsatellites shows that the young areas in the far eastern maria are associated with generally lower intensity remnant fields than the older areas. The young central area of Mare Smythii, the young western part of Mare Marginis, and the young and intermediate age areas in Mare Crisium have lower fields than do the older areas in each of the maria. The general association of older units with higher remnant magnetic fields has been previously noted by Soderblom and others (1977). They suggest that this relationship is due to a continuous decline of a primordial lunar magnetic field. The new data presented here and those of Lin and others (1977) suggest that this general relationship holds for all major maria units.

The Apollo γ-ray spectrometer data provides a measure of the relative elemental abundance of Th, K, U, Fe, and Ti (Arnold and others, 1977).

Correlation of the two data sets shows that maria of all ages in Mare Smythii and southern Mare Crisium have relatively low natural radioactivity or abundances of Th, K, and U compared to the western maria, particularly the Mare Imbrium area. These new data suggest that there is an east-west dichotomy in Th, K, and U abundance in mare basalts and that the presence of these elements is not correlated with age. This dichotomy could be caused by lateral heterogenity in the chemistry of the lunar crust, as suggested by Soderblom and others (1977). The areas of high natural radioactivity are associated with the Imbrium basin (the basin ejecta and the mare basalts). This association suggests that the rocks beneath the Imbrium basin, which are sources of the basin ejecta and the basalts, may contain more Th, K, and U than most other areas on the Moon. Additionally, the presence of young lava flows in both the eastern and western maria suggest that the relative abundance of radioactive elements measured from orbit (Th, K, U) have played only a minor role in the control of the duration and location of mare volcanic activity.

The Apollo X-ray spectrometers also provide information about the relative abundance of Fe and Ti (Bielefeld and others, 1976). Comparison of these data and the new age data shows that the old central part of Mare Crisium and the young central part of Mare Smythii have high Fe and Ti abundances than the intermediate age units on the edges of these basins. This correlation is consistent with that noted by Soderblom and others (1977) for other maria which they interpret to result from magma generation at different depths in the Moon.

The ratio of Mg to Al for lunar areas was measured by the Apollo 15 and 15 fluorescent X-ray spectrometer (Bielefeld and others, 1977). A comparison of these data and the age data show that the young central unit in Mare Smythii and the older central unit in Mare Crisium have relatively high Mg/Al ratios, whereas the intermediate units on the basin edges have lower Mg/Al ratios.

The new age data presented here and those of Boyce (1976) and Boyce and Johnson (1977) generally support earlier observations (Boyce and Dial, 1975) that (1) older units (older than about 3.5 b.y.) are generally found around the edges of the basins and (2) younger units (younger than about 3.5 b.y.) are generally in the centers. This pattern is thought to be the result of central subsidence of basins caused by isostatic adjustment to the weight of the lava and to subsurface evacuation and subsequent collapse as the lavas were extruded (Baldwin, 1963; Quaide, 1965; Howard and others, 1973; Boyce and Dial, 1975; Solomon and Head, 1978; Maxwell, 1978).

However, vents for very young flows (2.5 $\pm$ 0.05 b.y.) are generally located along the edge of basins, as the distribution of relative age units and photogeologic evidence show. Some young flows, such as those in Mare Imbrium that occupy large areas (> 3500 km^2), can be traced from their termination in the middle of basins back to their source on the edge (Schaber, 1973; Schaber and others, 1976). The large young flows without obvious traceable flow features, such as in western Mare Serenitatis (Thompson and others, 1973) and Mare Smythii, show embayment relations (based on age distribution and remote sensing data) that suggest that the flow originated on the edge and flowed toward the middle of the basins. Young flows (< 3500 km^2) of limited extent are found only on the edges of the basins; although some small, isolated, very young flows in the middle of some basins could be buried by large young flows, it is unlikely that all of these small flows were buried. Therefore, because large young flows can be shown to originate along basin edges and the small younger flows occur only on the edge of basins, we conclude that the vents for these very young flows are generally located on the edge of the basins.

Oceanus Procellarum, the exception, contains large areas of the youngest flow sequence with a significant area in the middle of the mare. Some of these flows clearly have their source in the middle (e.g., the flow around the Marius Hills), others may have originated at the edge. Oceanus Procellarum may be a composite of several ancient basins and the vents for the youngest flows may lie on the edges of these buried basins, or the mare lavas in Oceanus Procellarum may be too thin to cause significant isostatic subsidence.

Solomon and Head (1978) and Muehlberger (personal communication, 1978) suggest, on the basis of tectonic models, that the most likely eruptive sites in later stages of mare filling should be near the basin edges. They indicate that fractures which can act as magma conduits should be held open longer along the basin edges than elsewhere because tensional stress is generated at the basin edges by uncompensated mare loading. The age distributions presented here for the far eastern maria and those of Boyce (1976) provide empirical support to these models.

Summary

The emplacement of the far eastern maria occurred over an interval of about 1.25 aeons (from $\sim$ 3.75 b.y. to $\sim$ 2.5 b.y.) with extensive young

($\sim$2.5 $\pm$ 0.5 b.y.) mare occurring in all three far eastern maria. The relative ages determined here on the basis of crater density can be compared directly with the relative ages determined by Soderblom and Lebofsky (1972) and Boyce (1976) on the basis of crater morphology. The distribution of relative age units derived using these techniques show that the relationship suggested by Boyce and Dial (1975)--that, in general, the old mare units (> 3.5 b.y.) are found around the basin edges and the young mare units (< 3.5 b.y.) are found in the centers of basins--is valid for all major lunar maria. This comparison also shows that the youngest flows ($\sim$2.5 $\pm$ 0.5 b.y.) have their source vents on the edges of the maria basins--a fact that supports tectonic models that indicate tensional stress is generated on the basin edges due to uncompensated mare loading.

Data from instruments aboard the Apollo spacecrafts are the major source of information about the physical and chemical characteristics of the far eastern maria. Data from these instruments correlated with the relative age data presented here show that: (1) the young units in the far eastern maria have lower remnant magnetism than do the older units--a relationship that generally holds for all lunar maria (Soderblom and others, 1977); (2) the relatively lower natural radioactivity for all age units in the far eastern maria than for the western maria suggests that the relative abundance of these elements was only a minor factor in control of duration and location of maria volcanism. The non-uniform distribution of radioactive elements as determined from orbit may be due to lateral heterogeneity in the lunar crust, with the rocks beneath part of the western maria (notably Mare Imbrium) containing relatively more Th, K, and U than other areas; and (3) the abundance of Fe and Ti and the ratio of Mg to Al show that the old and young units in the far eastern maria are rich in Fe and Ti and have high Mg/Al ratios. The intermediate age units have lower Fe and Ti abundances and lower Mg/Al ratios.

Acknowledgements

I wish to thank G. Schaber for his critical review and D. A. Johnson for her technical assistance. I am especially indebted to Eric Eliason for his help with computer processing. This work was done under NASA contracts W 13-130 and W 13-709.

References

Arnold, J. R., Metzger, A. E. and Reedy, R. C., 1977, Computer-generated maps of lunar composition from gamma-ray data: Proceedings Lunar Science Conference Eighth, Geochimica et Cosmochimica Acta, Supp. 8, v. 1, p. 945-948.

Baldwin, R. B., 1963, The Measure of the Moon: University of Chicago Press, 488 p.

_____1969, Absolute ages of the lunar maria and large craters, I: Icarus, v. 11, p. 167-179.

Bielefeld, M. J., Andre, C. G., Eliason, E. M., Clark, P. E., Adler, I., and Trombka, J. I., 1976, Surface chemistry of selected lunar regions: Proceedings Lunar Science Conference Seventh, Geochimica et Cosmochimica Acta, Supp. 7, v. 3, p. 2661-2676.

Boyce, J. M., 1976, Ages of flow units in the lunar nearside maria based of Lunar Orbiter V photographs: Proceedings Lunar Science Conference Seventh, Geochimica et Cosmochimica Acta, Supp. 7, v. 3, p. 2717-2728.

Boyce, J. M., and Dial, A. L., Jr., 1975, Relative ages of flow units in Mare Imbrium and Sinus Iridum: Proceedings Lunar Science Conference Sixth, Geochimica et Cosmochimica Acta, Supp. 6, v. 3, p. 2585-2595.

Boyce, J. M. and Johnson, D. A., 1977, Ages of flow units in Mare Crisium based on crater density: Proceedings Lunar Science Conference Eighth, Geochimica et Cosmochimica Acta, Supp. 8, v. 3, p. 3495-3502.

Boyce, J. M., Schaber, G. G. and Dial, A. L., Jr., 1977, Age of Luna 24 mare basalts based on crater studies: Nature, no. 265, p. 38-39.

Drozd, R. J., Hohenburg, C. M., Morgan, C. J., and Ralston, C., 1974, Cosmic-ray exposure history at the Apollo 16 and other lunar sites: Lunar surface dynamics: Geochimica et Cosmochimica Acta, no. 38, p. 1625-1642.

Eliason, E. M. and Soderblom, L. A., 1977, An array processing system for lunar geochemical and geophysical data: Proceedings Lunar Science Conference Eighth, Geochimica et Cosmochimica Acta, Supp. 8, v. 3, p. 1163-1172.

Evensen, N. M., Murthy, V. R. and Coscio, M. R., Jr., 1973, Taurus-Littrow: Age of mare volcanism; chemical and Rb-Sr isotopic systematics of the dark mantle soil: American Geophysical Union Transactions EOS, v. 54, no. 6, p. 587-588.

Greeley, R. and Gault, D. E., 1970, Precision size-frequency distributions of craters for 12 selected areas on the lunar surface: The Moon, v. 2, p. 10-77.

Hartmann, W. K., 1970, Lunar cratering chronology: Icarus, v. 13, p. 299-301.

Howard, K. A., Carr, M. H., and Muehlberger, W. R., 1973, Basalt stratigraphy of southern Mare Serenitatis, in Apollo 15 Preliminary Science Report, NASA SP-330, p. 29-1 to 29-12.

Johnson, T. V., Mosher, J. A. and Matson, D. L., 1977, Lunar spectral units: A northern hemispheric mosaic: Proceedings Lunar Science Conference Eighth, Geochimica et Cosmochimica Acta, Supp. 8, v. 1, p. 1013-1028.

Lin, R. P., Anderson, K. A., Bush, R., and McGuire, R. E., 1976, Lunar surface magnetic fields detected by the electron reflection method: Proceedings Lunar Science Conference Seventh, Geochimica et Cosmochimica Acta, Supp. 7, v. 3, p. 2691-2703.

Lin, R. P., Anderson, K. A., Russell, C. T., Boyce, J. M., Masursky, H., and Wilhelms, D. E., 1977, Correlations of lunar surface remanent magnetic fields to surface geologic age, in Lunar Science VIII, v. 1, p. 14-15, The Lunar Science Institute, Houston.

Lucchitta, B. K., and Sanchez, A. G., 1975, Crater studies in the Apollo 17 region: Proceedings Lunar Science Conference Sixth, Geochimica et Cosmochimica Acta, Supp. 6, v. 3, p. 2427-2442.

Marti, K., Lightner, B. O., and Olson, T. W., 1973, Krypton-Xenon in the lunar samples and the age of North Ray Crater: Proceedings Lunar Science Conference Fourth, Geochimica et Cosmochimica Acta, Supp. 4, v. 3, p. 2037-2048.

Maxwell, T. A., 1978, A finite-element model of multi-ring basin ridge systems (abs.), in Lunar and Planetary Science IX, Lunar and Planetary Institute, Houston, Texas, v. 2, p. 708-710.

McCord, T. B., 1968, Color differences on the lunar surface: Ph.D. Thesis, California Institute of Technology, Pasadena, CA.

Morris, E. C. and Shoemaker, E. M., 1969, Craters, in Surveyor Project Final Report, Part II. Science Results: Jet Propulsion Laboratory Technical Report 32-1265, p. 65-69.

Neukum, G., Konig, B., and Arkani-Hamed, J., 1975, A study of lunar impact crater size-distributions: The Moon, v. 12, p. 201-230.

Neukum, G., Fechtig, H., Konig, B., Hiller, K., Wise, D. U., 1977, Lunar and martian cratering studies, and Mars Mariner 9 geologic mapping: NASA TMX-3511, p. 81-84.

Papanastassiou. D. A. and Wasserburg, G. J., 1971a, Lunar chronology and evolution from Rb-Sr studies of Apollo 11 and 12 samples: Earth Planetary Science Letters, v. 11, no. 37, p. 37-62.

Pieters, D. M., 1978, Mare basalt type on the frontside of the moon: Proceedings Lunar and Planetary Science Conference Ninth, Geochimica et Cosmochimica Acta, in press.

Quaide, W., 1965, Rilles, ridges, and domes-clues to maria history: Icarus, v. 4, p. 374-389.

Schaber, G. G., 1973, Eratosthenian volcanism in Mare Imbrium: Source of youngest lava flows, in Apollo 17 Preliminary Science Report, NASA SP-330, p. 30-17 to 30-25.

Schaber, G. G., Boyce, J. M., and Moore, H. J., 1976, The scarcity of mappable flow lobes on the lunar maria: Unique morphology of the Imbrium flows: Proceedings Lunar Science Conference Seventh, p. 2783-2800.

Shorthill, R. W., 1973, Infrared atlas charts of the eclipsed moon: The Moon, v. 7, p. 22-45.

Soderblom, L. A., Arnold, J. R., Boyce, J. M., and Lin, R. P., 1977, Regional variations in the lunar maria: Age, radioactivity, remanent magnetism: Proceedings Lunar Science Conference Eighth, Geochimica et Cosmochimica Acta, Supp. 8, v. 1, p. 1191-1200.

Soderblom, L. A., and Boyce, J. M., Distribution and evolution of global color provinces on the moon (abs.), in Lunar Science VII, The Lunar Science Institute, Houston, Texas, v. 2, p. 822-824.

Soderblom, L. A., and Lebofsky, L. A., 1972, Technique for rapid determination of relative ages of lunar areas from orbital photography: Journal Geophysical Research, v. 77, no. 2, p. 279-296.

Solomon, S. C., and Head, J. W., 1978, Vertical movement in mare basins: Relation to mare emplacement, basin tectonics, and lunar thermal history (abs.), in Lunar and Planetary IX, The Lunar and Planetary Institute, Houston, Texas, v. 2, p. 1080-1083.

Thompson, T. W., 1970, Map of radar reflectivity at 7.5m wavelength: Icarus, v. 13, no. 3, p. 363-370.

Thompson, T. W., Howard, K. A., Shorthill, R. W., Tyler, G. L., Zisk, S. H., Whitaker, E. A., Schaber, G. G., and Moore, H. J., 1973, Remote sensing of Mare Serenitatis, in Apollo 17 Preliminary Science Report, NASA SP-330, p. 33-3 to 33-9.

Wasserburg, G. J., and Papanastassiou, D. A., 1971, Age of an Apollo 15 mare basalt: Lunar crust and mantle evolution: Earth Planetary Science Letters, v. 13, no. 1, p. 97-104.

Whitaker, E. A., 1972, Lunar color boundaries and their relationship to topographic features: A preliminary report: The Moon, v. 4, p. 348-355.

Young, R. A., 1975, Mare crater size-frequency distributions: Implications for relative surface ages and regolith development: Proceedings Lunar Science Conference Sixth, Geochimica et Cosmochimica Acta, Supp. 6, v. 3, p. 2645-2662.

Zisk, S. H., and Hagfors, T., 1970, Radar atlas of the Moon, final report: Massachusetts Institute of Technology, Lincoln Laboratory, Cambridge, MA.

Appendix I

Crater density data for Mare Crisium including the number of craters greater than 900m diameter in each sample cell (cell size 256 km^2), and the center coordinates (latitude and longitude) of each cell.

APPENDIX I

Crater density data for Mare Crisium. Cell size for each sample area is 256 Km^2.

No. of Craters	Lat.	Long.	No. of Craters	Lat.	Long.
1	13.8	62.6	3	13.9	63.2
4	14.9	62.7	4	14.4	63.2
3	15.3	62.8	2	15.0	63.3
3	15.8	62.8	1	15.4	63.3
3	16.1	62.8	1	15.9	63.3
3	16.1	62.3	3	16.3	63.3
3	16.6	62.3	2	12.6	63.1
3	14.2	62.0	3	13.1	63.1
1	14.8	62.0	3	13.5	63.2
3	15.2	62.1	0	14.3	63.3
2	15.6	62.2	4	14.4	63.1
2	16.3	61.9	3	14.8	63.1
4	14.1	61.5	1	11.6	62.4
3	14.7	61.5	0	12.0	62.5
2	15.0	61.5	3	12.5	62.5
2	15.5	61.5	3	13.0	62.5
2	15.8	61.3	2	13.4	62.5
2	16.3	61.3	1	13.9	62.5
6	14.0	60.8	3	14.4	62.5
5	14.4	60.8	2	14.7	62.5
6	14.9	60.8	1	11.0	61.9
2	15.3	60.9	1	11.5	61.9
3	15.7	60.9	1	11.9	62.0
0	16.1	61.0	3	12.4	62.0
4	13.9	60.2	1	12.8	62.1
4	14.4	60.2	1	13.3	62.1
0	14.8	60.2	3	11.0	61.5
1	15.1	60.3	2	11.3	61.4
1	15.6	60.4	1	11.8	61.5
5	14.7	66.0	3	12.3	61.6
1	15.4	66.0	1	12.8	61.7
2	15.9	66.0	3	13.3	61.8
3	14.8	65.6	1	14.2	62.0
4	15.4	65.6	2	14.7	62.0
1	15.8	65.6	2	12.6	55.2
1	16.1	65.7	1	13.0	55.2
0	14.7	65.1	0	11.2	54.5
0	15.3	65.2	3	11.5	54.6
0	15.8	65.2	2	12.0	54.6
4	16.1	65.2	2	12.6	54.7
4	13.6	64.5	3	13.0	54.7
3	14.1	64.5	1	12.0	54.2
4	14.7	64.6	5	12.4	54.3
4	15.3	64.6	2	12.8	54.3
2	15.8	64.7	3	13.3	54.4
1	16.0	64.7	4	12.3	53.8
3	13.5	63.9	2	12.7	53.8
4	14.0	63.9	3	13.1	53.8
0	15.2	64.0	4	13.0	53.2
2	15.6	64.0	3	13.1	52.2
1	16.0	64.0	2	13.7	52.8

APPENDIX I (Continued)

Crater density data for Mare Crisium

No. of Craters	Lat.	Long.	No. of Craters	Lat.	Long.
2	13.5	52.3	1	10.9	56.7
3	14.0	52.9	0	11.3	56.8
1	14.0	52.3	0	11.8	56.9
3	14.5	52.8	4	12.2	56.9
3	14.9	52.9	4	12.6	56.9
3	14.5	52.4	4	13.0	57.0
2	14.9	52.4	3	13.5	57.0
0	14.3	51.7	5	14.0	57.2
0	14.3	51.4	4	14.4	57.2
0	14.7	51.7	6	14.8	57.2
1	14.7	51.4	0	10.3	56.2
4	12.9	56.5	2	10.7	56.3
3	13.3	56.5	3	11.2	56.3
3	13.8	56.5	0	11.5	56.3
4	14.2	56.6	2	12.0	56.4
4	14.8	56.6	2	12.4	56.4
3	15.1	56.6	3	13.6	59.0
0	10.2	55.8	4	14.0	59.0
1	10.6	55.8	2	14.8	59.1
1	11.0	55.8	2	15.3	59.2
0	11.4	55.9	2	15.7	59.2
2	12.0	56.0	2	10.7	58.1
4	12.4	56.0	4	11.1	58.2
4	12.9	56.0	2	11.6	58.2
2	13.2	56.1	3	12.0	58.2
3	13.7	56.2	1	12.5	58.3
4	14.2	56.2	2	13.0	58.4
4	14.6	56.3	2	13.4	58.4
2	15.0	56.3	3	14.2	58.5
6	10.6	55.4	3	14.6	58.5
0	10.9	55.4	4	15.2	58.6
1	11.4	55.4	3	15.6	58.7
1	11.8	55.4	3	10.6	57.7
3	12.2	55.5	1	11.0	57.7
1	12.7	55.5	0	11.5	57.7
0	10.8	54.9	3	12.0	57.8
1	11.2	54.9	3	12.4	57.9
0	11.6	54.9	0	12.9	58.0
1	12.1	55.1	3	13.3	58.0
2	10.5	57.1	2	13.8	58.1
1	10.9	57.2	2	14.3	58.1
4	11.4	57.3	2	14.6	58.2
1	11.8	57.4	4	15.0	58.2
3	12.8	57.5	4	15.5	58.3
3	13.2	57.5	0	14.2	59.9
5	13.6	57.6	0	21.4	55.6
1	14.1	57.7	2	21.8	55.6
4	14.5	57.8	2	21.5	55.8
4	15.0	57.8	1	21.8	55.8
5	15.4	57.8	2	21.6	56.2
1	10.4	56.6	2	21.9	56.2

APPENDIX I (Continued)

Crater density data for Mare Crisium

No. of Craters	Lat.	Long.	No. of Craters	Lat.	Long.
0	21.6	56.8	4	21.5	54.0
4	22.0	56.8	3	20.9	62.6
3	21.8	57.8	1	21.4	62.7
0	22.2	57.8	5	21.2	63.1
0	21.9	58.2	4	21.5	63.2
3	22.3	58.3	0	21.3	64.2
3	22.0	58.6	0	19.8	51.8
2	22.1	58.7	1	19.9	52.2
2	22.1	59.1	4	20.5	52.2
5	22.6	59.1	4	20.1	52.9
2	22.1	59.6	2	20.2	54.0
1	22.6	59.6	4	20.7	54.0
1	22.1	60.2	3	20.4	54.6
2	22.5	60.2	1	20.9	54.6
4	22.1	55.3	1	20.6	55.3
3	22.2	55.9	2	21.0	55.3
1	22.3	56.3	2	20.6	55.8
3	22.7	58.3	5	21.0	55.8
2	22.9	59.1	1	13.2	64.3
1	23.2	58.8	3	13.7	64.4
1	22.9	59.1	3	14.2	64.5
1	22.8	58.8	1	12.7	64.1
2	23.2	60.1	0	13.2	64.1
1	20.8	56.2	3	13.6	64.2
3	21.2	56.2	2	14.1	64.2
1	20.8	56.6	1	12.3	63.6
3	21.3	56.7	3	12.6	63.7
1	20.9	57.0	1	13.5	63.8
1	21.4	57.0	1	14.0	63.8
0	21.0	57.6	0	11.8	62.9
0	21.4	57.7	2	12.1	63.1
3	21.1	58.1	0	10.7	59.5
3	21.5	58.2	1	11.0	59.5
5	21.2	58.5	1	11.4	59.5
1	21.6	58.6	2	11.9	59.6
3	21.2	59.0	2	12.4	59.6
0	21.6	59.1	2	12.9	59.7
1	21.5	59.4	1	13.4	59.7
2	21.7	59.5	0	13.9	59.8
1	21.5	60.0	4	14.6	59.9
4	21.8	60.1	2	15.0	59.9
2	21.8	62.7	1	10.9	59.0
0	21.6	62.1	0	11.4	59.1
3	21.5	61.6	0	11.8	59.1
2	22.0	61.6	3	12.2	59.2
1	21.5	60.5	2	12.7	59.2
2	21.9	60.5	2	13.1	59.2
2	21.5	61.0	2	13.6	59.2
4	20.9	52.2	2	14.2	59.3
4	21.4	53.3	3	14.5	59.4
3	21.1	54.0	2	15.0	59.4

APPENDIX I (Continued)

Crater density data for Mare Crisium

No. of Craters	Lat.	Long.
2	15.3	59.5
1	15.8	59.6
2	10.8	58.6
5	11.2	58.6
2	11.6	58.7
2	12.2	58.7
2	12.6	58.8
1	13.0	58.9
4	11.4	61.0
2	11.8	61.1
2	12.2	61.1
1	12.8	61.2
3	13.2	61.2
3	13.7	61.2
4	14.1	61.2
4	14.6	61.3
1	10.3	59.8
1	11.2	60.5
3	11.6	60.5
0	12.1	60.6
2	12.7	60.6
3	13.1	60.7
1	13.6	60.7
1	14.0	60.7
4	14.4	60.7
1	10.7	59.9
2	11.1	59.9
0	11.5	59.9
3	12.0	60.0
1	12.5	60.1
2	13.0	60.2
3	13.5	60.2
1	14.0	60.2
1	14.4	60.2
2	14.8	60.3
4	15.2	60.2
4	18.5	51.7
4	17.5	51.8
2	18.0	51.8
3	19.3	51.7
5	18.9	51.7
4	19.6	52.8
3	16.7	52.4
1	17.2	52.4
5	17.6	52.3
4	18.1	52.3
4	18.6	52.3
1	19.0	52.3
4	19.5	52.3
1	17.3	52.8
4	18.8	52.8
1	19.2	52.8
2	16.5	53.3
4	17.0	53.3
2	17.4	53.3
1	16.7	53.9
3	17.1	53.9
1	17.6	54.0
1	18.9	54.0
4	19.4	53.9
3	19.8	53.9
0	17.7	54.5
1	18.2	54.5
4	18.6	54.5
2	19.0	54.4
2	19.2	54.5
2	20.0	54.5
2	17.4	55.1
1	17.9	55.1
0	18.3	55.0
1	18.7	55.0
2	19.2	55.0
0	19.7	55.0
3	20.1	55.1
2	22.5	56.3
1	22.9	56.3
2	23.0	56.6
0	22.7	57.2
2	23.0	57.2
0	23.1	57.7
1	23.8	58.4
1	23.0	59.0
1	23.4	59.0
1	23.8	59.0
3	16.6	55.5
0	17.1	55.5
3	17.5	55.5
3	18.5	55.5
2	18.9	55.5
0	19.3	55.5
4	19.8	55.5
0	20.3	55.5
1	16.7	55.9
2	17.1	56.0
4	17.6	56.0
4	18.1	56.0
0	18.5	55.9
7	19.0	55.9
2	19.5	55.9
0	19.9	55.9
1	20.4	55.9
3	16.7	56.3

APPENDIX I (Continued)

Crater density data for Mare Crisium

No. of Craters	Lat.	Long.	No. of Craters	Lat.	Long.
1	18.1	56.3	5	22.4	58.6
5	21.0	56.3	2	16.3	59.1
2	19.1	56.3	6	16.8	59.1
2	19.5	56.3	2	17.3	59.1
5	20.0	56.3	5	17.8	59.1
1	20.4	56.3	1	18.3	59.1
4	16.8	56.7	0	18.7	59.1
2	17.3	56.7	1	19.1	59.1
3	17.7	56.7	3	19.7	59.1
3	18.2	56.7	3	20.0	59.1
1	15.6	56.7	2	20.2	59.2
4	19.1	56.7	4	18.5	59.6
0	19.6	56.7	2	19.0	59.5
2	16.5	57.2	2	19.4	59.5
4	16.9	57.2	2	19.9	59.4
1	17.4	57.2	3	21.0	60.1
3	17.9	57.2	1	21.2	60.4
4	18.3	57.2	4	18.4	59.4
0	18.8	57.2	1	18.8	59.4
2	19.2	57.1	0	19.2	59.4
4	19.7	57.1	3	19.7	59.5
1	20.6	57.2	2	20.1	59.5
1	16.6	57.7	1	20.4	59.6
8	17.0	57.7	2	20.9	59.6
1	17.5	57.7	3	16.6	60.1
3	18.0	57.7	2	17.1	60.1
2	19.8	57.7	2	17.6	60.1
1	20.2	57.8	2	18.0	60.1
1	20.6	57.8	2	18.5	60.1
5	16.7	58.2	6	18.9	60.2
2	17.2	58.2	1	19.4	60.1
4	17.6	58.2	0	20.2	60.2
2	18.1	58.2	4	20.6	60.1
1	18.6	58.3	2	16.7	60.4
3	19.0	58.3	2	17.2	60.5
1	19.4	58.3	1	17.6	60.5
2	19.8	58.3	0	18.1	60.3
1	20.3	58.3	1	18.6	60.3
2	20.7	58.3	1	19.0	60.3
3	22.0	58.3	2	19.4	60.4
2	22.3	58.3	4	19.9	60.5
3	16.8	58.6	2	20.3	60.4
3	17.3	58.6	2	20.7	60.4
3	17.8	58.6	1	16.4	60.8
4	18.1	58.6	2	16.8	60.8
2	15.8	58.7	0	17.3	60.8
3	18.9	58.7	3	17.8	60.9
2	19.9	58.7	0	18.2	60.9
4	20.3	58.6	2	18.6	60.9
1	20.7	58.6	1	19.1	61.0
2	22.0	58.6	2	19.5	61.0

APPENDIX I (Continued)

Crater density data for Mare Crisium

No. of Craters	Lat.	Long.	No. of Craters	Lat.	Long.
3	19.9	60.9	1	21.5	62.9
4	20.4	60.9	2	16.2	63.2
2	20.7	60.9	3	16.7	63.2
2	21.2	61.0	2	17.2	63.2
2	16.4	61.3	1	17.7	63.3
1	16.9	61.3	0	18.1	63.3
0	17.4	61.3	1	18.6	63.3
1	17.8	61.3	0	19.1	63.3
1	18.3	61.3	2	19.5	63.4
1	18.7	61.3	0	19.9	63.4
2	19.2	61.3	0	20.7	63.4
1	19.6	61.3	4	16.0	63.7
1	20.0	61.3	5	16.5	63.7
2	20.4	61.4	1	16.9	63.7
0	20.8	61.4	1	17.4	63.8
0	21.3	61.4	3	17.8	63.8
0	22.1	61.4	2	18.2	63.8
3	22.1	61.9	0	18.7	63.8
1	16.5	61.8	0	19.3	63.9
3	16.9	61.8	0	19.6	63.9
1	17.4	61.8	0	20.0	63.9
2	17.9	61.8	0	20.5	63.9
1	18.3	61.8	1	20.9	64.0
2	18.8	61.8	1	21.2	64.0
1	19.2	61.8	2	16.1	64.2
1	19.8	61.8	1	16.5	64.2
1	20.1	61.9	3	16.9	64.2
1	20.5	61.9	2	17.4	64.2
2	16.6	62.3	1	17.8	64.2
1	17.0	62.3	1	18.3	64.2
2	17.5	62.3	0	18.8	64.3
0	18.0	62.3	0	19.3	64.3
3	18.5	62.3	1	19.7	64.3
0	18.9	62.3	1	20.0	64.3
5	19.4	62.3	3	18.8	51.3
3	19.7	62.3	4	19.3	51.3
2	20.2	62.4	3	16.5	51.8
5	20.6	62.3	6	17.0	51.8
2	21.8	62.4	0	17.9	51.2
2	22.2	62.4	1	20.5	64.3
1	16.3	62.7	0	20.9	64.4
1	16.7	62.7	2	16.2	64.7
3	17.1	62.7	3	16.6	64.7
0	17.6	62.7	2	17.0	64.7
3	18.0	62.7	2	17.5	64.7
2	18.5	62.8	1	17.9	64.7
2	18.9	62.8	1	18.4	64.7
2	19.4	62.8	0	18.8	64.8
2	19.8	62.8	1	19.3	64.8
2	20.3	62.8	0	19.6	64.8
0	20.7	62.8	0	20.2	64.7

APPENDIX I (Continued)

Crater density data for Mare Crisium

No. of Craters	Lat.	Long.
1	20.6	64.7
1	20.9	64.8
0	16.3	65.3
2	16.6	65.3
1	17.0	65.2
2	17.5	65.3
0	18.3	65.3
0	20.5	66.0
6	18.5	65.2
1	18.8	65.2
0	19.4	65.2
1	19.7	65.3
1	20.2	65.3
0	20.6	65.3
2	16.3	65.6
5	16.6	65.6
3	17.1	65.6
2	17.5	65.6
2	18.0	65.7
5	18.5	65.7
0	18.9	65.8
1	19.4	65.9
1	19.8	66.0
2	16.6	66.1
1	17.0	66.1
1	17.4	66.2
2	17.8	66.3
3	18.1	66.4
5	18.7	66.5
1	19.2	66.5
2	16.3	66.6
0	16.7	66.6
6	17.7	66.7
3	18.2	66.8
4	18.6	66.9
1	19.2	66.9
0	19.6	67.0
3	16.4	67.6
4	16.8	67.5
1	17.3	67.3
3	17.8	67.4
0	18.2	67.5
2	18.7	67.6
2	15.6	68.0
1	16.0	67.9
3	16.3	67.9
4	14.9	67.5
3	15.6	67.5
5	16.0	67.5
7	16.3	67.5
4	14.9	67.0
1	15.5	67.0
2	15.9	67.0
3	16.3	67.0
2	14.8	66.4
2	15.4	66.4
2	15.9	66.5
4	16.2	66.5
2	16.3	52.8
3	14.0	52.2
3	14.4	52.2
3	14.8	52.2
3	15.2	52.2
3	15.7	52.2
1	16.2	52.2
0	14.3	51.8
0	14.3	51.4
0	14.6	51.8
1	14.6	51.3
4	15.6	51.8
2	16.2	51.7
3	14.5	56.2
3	15.0	56.2
4	15.4	56.2
1	15.8	56.3
3	16.3	56.3
3	15.3	55.9
2	15.8	55.9
1	16.2	55.9
2	16.1	55.5
3	15.5	53.5
2	16.0	53.5
0	14.5	52.7
2	14.9	52.8
4	15.4	52.8
1	15.9	52.8
4	16.0	58.7
2	16.5	58.7
4	13.8	58.0
3	14.2	58.1
2	14.6	58.1
4	15.0	58.1
4	15.4	58.2
4	15.8	58.2
1	16.4	58.3
0	14.1	57.6
1	14.5	57.7
3	14.9	57.7
5	15.4	57.7
4	15.8	57.8
3	16.3	57.8
5	13.9	57.0

APPENDIX I (Continued)

Crater density data for Mare Crisium

No. of Craters	Lat.	Long.	No. of Craters	Lat.	Long.
8	14.4	57.1			
4	14.8	57.1			
2	15.7	57.2			
3	16.1	57.3			
3	13.8	56.5			
3	14.2	56.6			
4	14.6	56.6			
2	15.5	56.7			
1	16.0	56.7			
3	16.4	56.7			
1	13.7	56.1			
3	14.1	56.1			
3	16.0	60.5			
3	16.5	60.5			
3	13.8	59.8			
4	14.2	59.8			
3	14.6	59.8			
2	15.0	59.8			
2	15.4	59.9			
4	15.9	59.9			
1	16.4	60.1			
4	13.7	59.3			
4	14.1	59.4			
3	14.5	59.4			
2	14.9	59.4			
0	15.4	59.5			
1	15.8	59.5			
0	16.2	59.6			
3	13.6	58.9			
4	13.9	58.9			
2	14.3	59.0			
2	14.8	59.0			
1	15.3	59.0			
2	15.7	59.1			
3	16.1	59.1			
1	13.8	58.5			
1	14.3	58.5			
3	14.7	58.6			
2	15.2	58.6			
3	15.5	58.7			

Appendix II

Crater density data for Mare Marginis including the number of craters greater than 900m diameter in each sample (cell size 153 km^2) and the center coordinates (latitude and longitude) of each cell.

APPENDIX II

ter density data for Mare Marginis. Cell size for each sample area is 153 Km^2.

No. of Craters	Lat.	Long.	No. of Craters	Lat.	Long.
1	12.8	87.5	4	14.1	85.9
1	13.2	87.6	2	13.7	85.9
1	13.6	87.6	3	13.3	85.9
1	14.0	87.6	2	12.9	85.8
2	17.0	87.8	4	12.6	85.8
1	17.3	87.8	4	12.2	85.7
4	17.6	87.8	2	13.8	85.6
1	11.7	86.9	1	11.8	85.3
0	12.1	86.9	0	17.7	86.7
0	12.5	87.0	0	17.4	86.7
2	12.9	87.0	2	17.0	86.6
0	13.2	87.0	1	16.7	86.6
0	13.6	87.0	1	16.3	86.5
2	14.0	87.0	0	16.0	86.5
1	14.4	87.1	3	15.6	86.4
3	14.8	87.1	1	15.2	86.4
1	15.3	87.1	3	14.9	86.4
0	16.2	87.3	0	14.5	86.3
1	16.6	87.3	1	14.1	86.3
4	17.0	87.3	1	13.7	86.2
0	17.4	87.4	2	13.3	86.2
1	17.7	87.4	1	12.9	86.1
2	11.8	86.4	3	12.6	86.1
3	17.2	85.4	1	12.2	86.0
0	16.8	85.4	2	11.8	86.0
1	16.4	85.3	1	18.1	87.0
2	15.0	85.2	2	17.7	87.0
0	14.6	85.2	1	17.4	87.0
1	14.1	85.1	0	17.0	86.9
1	13.7	85.1	1	16.6	86.9
3	13.3	85.1	2	16.3	86.8
0	13.0	85.0	0	15.9	86.8
0	12.7	85.0	4	12.1	86.4
1	17.2	85.8	0	12.5	86.5
0	16.8	85.8	1	12.9	86.5
0	16.8	85.8	0	13.2	86.5
1	16.4	85.7	1	13.6	86.6
0	15.3	85.6	0	14.0	86.6
1	15.0	85.6	2	14.4	86.6
1	14.6	85.6	3	14.8	86.7
1	14.1	85.5	2	15.1	86.7
3	15.7	85.5	2	15.5	86.7
3	15.3	85.5	1	12.1	82.4
2	14.9	85.4	0	11.7	82.3
0	14.5	85.4	1	18.1	83.2
1	17.8	86.4	0	17.7	83.2
0	17.5	86.2	0	17.4	83.1
1	15.6	86.2	3	17.0	83.1
1	15.2	86.1	1	16.6	83.1
1	14.9	86.0	1	16.2	83.1
1	14.5	86.0	0	15.8	63.0

APPENDIX II (Continued)

Crater density data for Mare Marginis.

No. of Craters	Lat.	Long.
0	15.4	83.0
1	15.0	83.0
1	14.7	83.0
0	14.4	83.0
0	14.0	82.9
0	12.5	83.0
0	12.1	82.8
1	11.7	82.8
0	18.1	83.5
1	17.7	83.5
1	17.3	83.4
1	16.9	83.4
0	16.5	83.4
1	16.1	83.4
4	15.7	83.4
0	15.3	83.3
1	15.0	83.3
1	14.6	83.3
1	14.2	83.3
0	13.9	83.2
0	12.8	83.2
0	12.5	83.2
2	12.1	83.1
1	18.1	83.8
2	17.7	83.8
0	17.3	83.7
1	16.9	83.7
1	16.5	83.7
1	16.1	83.7
0	13.7	83.6
3	15.0	83.6
1	14.6	83.6
3	14.2	83.6
0	13.8	83.5
2	13.5	83.5
0	13.2	83.5
2	12.9	83.5
0	12.5	83.4
1	12.1	83.4
0	14.0	85.2
1	13.7	85.1
3	13.4	85.1
1	13.1	85.1
0	12.7	85.0
0	12.3	85.0
2	11.9	85.0
1	17.0	85.7
0	16.6	85.7
1	16.3	85.6
1	15.0	85.6
2	14.7	85.6
1	14.3	85.6
1	14.0	85.5
3	13.7	85.5
1	13.4	85.5
2	13.0	85.4
2	12.6	85.4
0	12.3	85.4
2	11.9	85.4
1	17.8	86.2
0	17.4	86.2
1	15.4	86.1
0	15.0	86.1
1	14.6	86.0
1	14.3	86.0
4	14.0	85.9
2	13.6	85.9
2	13.3	85.9
2	13.0	85.8
4	12.6	85.8
3	12.3	85.8
2	11.9	85.7
2	8.2	84.4
0	7.9	84.4
0	10.1	84.9
2	9.8	84.9
0	9.5	84.8
0	10.0	85.2
1	9.7	85.2
3	9.4	85.1
0	10.0	85.7
1	9.6	85.6
1	9.2	85.5
0	10.2	84.8
3	9.8	84.8
0	9.4	84.7
4	8.2	84.7
0	7.9	84.6
1	10.1	85.2
1	9.7	85.2
4	9.3	85.2
0	8.9	85.1
0	8.5	85.1
3	8.1	85.1
0	7.8	85.0
0	10.0	85.6
1	9.7	85.6
2	9.3	85.6
1	8.9	85.5
3	8.5	85.5
1	8.1	85.5
0	7.8	85.5

APPENDIX II (Continued)

Crater density data for Mare Marginis.

No. of Craters	Lat.	Long.	No. of Craters	Lat.	Long.
0	8.7	85.9	3	12.7	89.1
0	8.3	85.9	3	12.4	89.1
0	8.0	85.8	2	16.0	89.7
0	9.4	83.4	1	15.7	89.7
0	9.8	83.4	2	15.3	89.6
0	9.4	83.7	2	14.9	89.6
0	9.0	83.7	0	14.6	89.6
0	8.6	83.7	3	14.3	89.6
0	9.4	84.1	3	13.0	89.5
0	9.0	84.1	0	17.3	88.2
1	8.6	84.0	1	12.5	87.5
0	10.2	84.6	0	12.1	87.4
0	9.8	84.6	1	11.7	87.4
0	9.4	84.6	1	12.7	89.4
2	9.0	84.5	2	12.3	89.4
0	8.6	84.5	4	15.6	89.9
1	15.6	88.6	5	15.2	89.9
2	11.7	87.8	1	14.9	89.8
3	12.1	87.8	0	14.6	89.8
5	12.5	87.9	2	13.0	89.7
6	12.5	87.9	1	12.6	89.7
0	12.9	87.9	2	12.2	89.7
3	13.2	88.0	1	15.5	90.1
1	13.6	88.0	0	15.2	90.1
2	15.3	88.6	1	14.9	90.1
5	15.0	88.5	0	12.6	90.0
2	14.6	88.5	0	12.2	90.0
0	13.5	88.4	0	11.9	90.0
3	13.1	88.4	2	12.6	90.3
4	12.8	88.4	1	12.2	90.3
1	12.4	88.3	1	11.9	90.2
2	12.0	88.3	3	12.6	90.6
4	11.6	88.3	0	12.2	90.6
0	16.1	89.0	0	11.8	90.5
0	15.7	89.0	2	11.4	90.5
1	15.3	88.9	2	12.6	91.0
2	15.0	88.9	0	18.4	84.1
2	14.6	88.9	0	18.0	84.1
2	14.3	88.9	0	17.6	84.1
1	13.3	88.8	0	17.3	84.0
2	13.0	88.8	2	16.9	84.0
5	12.7	88.8	4	16.5	84.0
3	12.4	88.7	2	16.1	83.9
2	12.0	88.7	1	15.7	83.9
1	16.1	89.4	1	15.2	83.9
0	15.7	89.3	0	14.9	83.9
3	15.3	89.3	2	14.6	83.8
3	15.0	89.3	3	14.2	83.8
0	14.6	89.2	1	13.9	83.8
2	14.3	89.2	0	13.6	83.7
5	13.0	89.2	1	13.2	83.7

APPENDIX II (Continued)

Crater density data for Mare Marginis.

No. of Craters	Lat.	Long.	No. of Craters	Lat.	Long.
1	12.8	83.7	1	17.0	85.6
1	12.4	83.7	1	16.6	85.5
0	12.0	83.7	0	16.2	85.4
1	18.0	84.5	0	14.8	85.3
2	17.6	84.5	0	14.0	82.5
1	17.2	84.4	0	14.4	82.5
1	16.9	84.4	0	14.7	82.5
2	16.5	84.4	0	15.0	82.5
1	16.0	84.4	0	16.6	82.6
0	15.6	84.3	2	17.0	82.7
2	15.2	84.3	1	17.4	82.7
0	14.9	84.3	0	17.8	82.7
0	14.6	84.2	1	14.5	81.7
1	14.2	84.2	1	18.2	82.8
2	13.9	84.2	1	11.3	81.7
1	12.6	84.2	1	11.7	81.8
1	13.6	84.2	1	11.3	82.0
1	13.2	84.1	1	11.7	82.0
0	12.8	84.1	1	12.1	82.0
1	12.4	84.1	1	14.1	82.1
1	12.0	84.1	2	14.5	82.2
1	17.9	84.8	0	14.9	82.2
0	17.6	84.8	0	17.5	82.2
0	17.2	84.8			
3	16.8	84.7			
0	16.4	84.7			
0	16.0	84.7			
0	15.6	84.6			
1	15.2	84.6			
0	14.8	84.6			
0	14.5	84.5			
1	14.2	84.5			
3	13.8	84.5			
0	13.5	84.5			
2	13.1	84.4			
1	12.4	84.4			
1	12.0	84.4			
2	17.0	85.1			
0	16.6	85.1			
1	16.2	85.0			
0	15.8	85.0			
0	15.5	85.0			
1	15.1	85.0			
1	14.8	85.0			
1	14.4	84.9			
1	14.1	84.9			
0	13.7	84.9			
0	13.4	84.9			
0	13.1	84.9			
1	12.7	84.9			
0	11.9	84.8			

Appendix III

Crater density data for Mare Smythii including the number of craters greater than 900m diameter in each sample cell (cell size 153 km^2), and the center coordinates (latitude and longitude) of each cell.

APPENDIX III

ter density data for Mare Smythii. Cell size for each sample is 153 Km^2.

No. of Craters	Lat.	Long.	No. of Craters	Lat.	Long.
1	3.6	88.5	1	-0.5	88.9
0	4.4	88.2	1	-1.0	88.9
0	4.0	88.2	1	-1.4	88.8
1	3.6	88.1	2	3.9	89.9
3	3.2	88.1	1	3.5	89.9
1	2.8	88.0	0	3.1	89.8
2	2.4	88.0	0	2.7	89.8
1	2.0	87.9	0	2.3	89.7
2	1.6	87.9	0	1.9	89.7
2	1.2	87.8	1	1.5	89.6
0	0.8	87.7	1	1.1	89.5
0	0.4	87.7	0	0.7	89.5
0	0.0	87.6	2	0.3	89.4
2	-0.5	87.6	1	-0.1	89.3
2	-0.9	87.5	1	-0.6	89.2
0	4.0	88.6	0	-1.0	89.2
1	3.2	88.5	2	3.5	85.1
1	2.8	88.5	0	3.5	85.4
0	2.4	88.4	0	3.1	85.3
1	2.0	88.4	0	4.1	86.0
0	1.6	88.3	0	3.8	85.9
1	1.2	88.3	0	3.5	85.8
0	0.8	88.2	2	3.0	85.7
1	0.4	88.2	0	2.5	85.6
0	0.0	88.1	2	2.1	85.5
2	-0.5	88.1	2	1.6	85.5
0	-0.9	88.0	1	4.1	86.5
1	4.0	88.9	1	3.8	86.4
0	3.2	88.8	1	3.4	86.3
0	2.8	88.8	1	2.9	86.3
1	2.4	88.7	1	2.4	86.2
0	2.0	88.7	0	2.0	86.1
1	1.6	88.7	0	1.6	86.0
1	1.2	88.6	2	4.4	86.8
1	0.8	88.6	2	4.1	86.7
1	0.4	88.6	0	3.8	86.7
0	0.0	88.5	1	3.4	86.6
0	-0.5	88.5	0	2.9	86.5
3	-1.0	88.5	1	2.4	86.5
2	-1.4	88.4	2	2.0	86.4
1	-1.7	88.4	1	1.6	86.4
0	3.9	89.3	0	1.3	86.3
0	3.2	89.2	3	4.1	87.0
0	2.8	89.2	0	3.8	87.0
0	2.4	89.1	1	3.4	86.9
0	2.0	89.1	1	2.0	86.7
1	1.6	89.0	1	1.6	86.6
0	1.2	89.0	0	1.2	86.6
1	0.8	89.0	0	0.8	86.5
1	0.4	88.9	1	0.3	86.5
0	0.0	88.9	0	0.0	86.5

APPENDIX III (Continued)

Crater density data for Mare Smythii.

No. of Craters	Lat.	Long.	No. of Craters	Lat.	Long.
0	-0.4	86.4	1	1.9	90.4
0	-0.8	86.3	0	1.5	90.3
1	0.4	86.1	1	1.1	90.2
1	0.0	86.0	0	0.8	90.2
3	-0.4	85.9	1	0.4	90.1
0	-0.8	85.8	0	4.1	91.2
0	4.3	87.5	0	3.8	91.1
1	4.0	87.4	0	3.5	91.0
1	3.7	87.4	1	3.1	91.0
2	3.4	87.3	0	2.6	90.9
1	2.5	87.2	0	2.2	90.9
2	2.0	87.2	0	1.8	90.8
2	1.7	87.1	1	1.4	90.7
0	1.3	87.0	0	1.0	90.7
0	0.8	87.0	1	0.6	90.6
0	0.4	86.9	2	0.2	90.6
0	0.0	86.9	1	-0.2	90.5
3	-0.4	86.8	1	4.1	91.5
0	-0.9	86.7	1	3.8	91.5
1	4.4	87.7	0	3.5	91.4
0	4.0	87.6	0	3.1	91.4
2	3.7	87.6	0	2.6	91.3
1	3.3	87.5	0	2.2	91.3
3	2.8	87.5	0	1.8	91.3
0	2.4	87.5	1	1.4	91.2
0	2.0	87.4	1	1.0	91.1
1	1.6	87.4	1	0.6	91.0
1	1.2	87.4	2	0.2	91.0
1	0.8	87.3	0	-0.2	90.9
0	0.4	87.2	2	-0.6	90.8
0	0.0	87.2	1	4.1	91.7
3	-0.4	87.2	2	3.8	91.7
2	-0.9	87.1	0	3.0	91.6
1	4.2	90.3	1	2.6	91.6
0	3.9	90.2	1	2.2	91.5
2	3.5	90.1	1	1.8	91.5
1	3.1	90.1	2	1.4	91.5
0	2.6	90.1	1	1.0	91.4
0	2.2	90.0	1	0.6	91.4
0	1.9	90.0	1	0.2	91.3
0	1.5	90.0	2	3.8	92.2
0	1.1	89.9	2	3.4	92.2
1	0.8	89.9	3	3.0	92.1
2	0.4	89.8	2	2.6	92.0
0	4.2	89.8	2	2.2	92.0
0	4.2	90.6	0	1.8	91.9
2	3.9	90.6	1	1.4	91.9
0	3.5	90.5	2	1.0	91.8
0	3.1	90.5	5	0.6	91.8
0	2.6	90.5			
0	2.2	90.4			

Appendix IV

Crater density data for Mare Humorum including the number of craters greater than 900m diameter in each sample cell (cell size 205 km^2), and the center coordinates (latitude and longitude) of each cell.

APPENDIX IV

Crater density data for Mare Humorum. Cell size for each sample is 205 Km^2.

No. of Craters	Lat.	Long.	No. of Craters	Lat.	Long.
1	21.5	34.1	1	20.5	35.9
1	21.0	34.2	1	20.2	35.9
3	20.6	34.2	1	19.5	36.0
0	20.2	34.2	1	19.1	36.0
0	19.9	34.3	0	23.8	36.0
1	19.5	34.3	2	23.4	36.0
3	23.6	34.3	1	23.0	36.0
4	23.2	34.3	0	22.5	36.1
2	22.8	34.4	1	22.1	36.1
0	22.4	34.4	0	21.7	36.1
2	22.0	34.5	0	21.3	36.2
1	21.5	34.5	1	20.9	36.2
2	21.0	34.5	0	20.5	36.2
3	20.6	34.6	2	20.1	36.3
2	20.3	34.6	0	19.8	36.3
0	20.0	34.6	1	19.5	36.3
2	19.6	34.7	3	19.2	36.4
2	19.3	34.7	4	18.8	36.4
1	23.7	34.7	4	21.4	37.5
0	23.3	34.7	1	21.0	37.6
3	22.9	34.8	1	20.6	37.6
4	22.5	34.9	2	20.2	37.6
0	22.0	34.9	0	19.9	37.6
2	21.5	35.0	0	19.6	37.7
2	21.1	35.0	0	19.3	37.7
1	20.7	35.0	1	18.9	37.7
1	20.3	35.1	2	23.8	37.8
1	20.0	35.1	0	23.4	37.8
2	19.7	35.1	1	23.0	37.8
2	19.4	35.2	1	22.6	37.8
1	23.8	35.2	2	22.2	37.9
1	23.4	35.2	0	21.8	37.9
0	23.0	35.3	2	21.4	38.0
2	22.6	35.3	3	21.0	38.0
0	22.2	35.3	2	20.6	38.0
1	21.8	35.4	1	20.3	38.0
1	21.3	35.4	3	20.0	38.1
0	20.9	35.4	0	19.6	38.1
1	20.5	35.5	1	19.3	38.1
0	20.2	35.5	2	23.8	38.2
0	19.9	35.5	2	23.4	38.2
0	19.5	35.5	3	23.0	38.2
1	19.1	35.6	3	22.6	38.3
5	23.8	35.6	0	22.2	38.3
2	23.4	35.6	1	21.8	38.4
1	23.0	35.6	1	21.4	38.4
2	22.6	35.7	3	21.0	38.4
3	22.2	35.7	5	20.6	38.5
1	21.8	35.8	0	20.3	38.5
0	21.3	35.8	1	20.0	38.5
1	20.9	35.9	0	19.6	38.6

APPENDIX IV (Continued)

Crater density data for Mare Humorum.

No. of Craters	Lat.	Long.
0	19.3	38.6
2	23.9	38.7
2	21.8	37.5
4	22.2	37.4
2	22.6	37.4
2	23.0	37.3
0	23.4	37.3
4	23.8	37.3
2	18.9	37.2
0	19.3	37.2
1	19.6	37.2
2	20.2	37.2
3	20.6	37.1
3	21.0	37.1
3	21.4	37.1
4	21.8	37.1
0	22.2	37.0
2	22.6	36.9
0	23.0	36.9
1	23.4	36.9
1	23.8	36.8
1	23.4	36.4
3	23.0	36.4
0	22.6	36.5
1	22.2	36.5
2	21.8	36.5
2	21.4	36.6
3	21.0	36.6
0	20.6	36.6
1	20.2	36.7
0	19.9	36.7
0	19.5	36.7
1	19.2	36.7
4	18.8	36.8
2	23.8	36.4
1	23.5	38.7
0	23.1	38.8
0	22.7	38.8
1	22.3	38.8
1	21.9	38.9
1	21.4	38.9
0	21.0	38.9
3	20.6	39.0
1	20.3	39.0
0	20.0	39.0
1	19.6	39.0
1	23.9	39.2
1	23.5	39.2
0	23.1	39.3
0	22.3	39.3

No. of Craters	Lat.	Long.
1	21.9	39.4
1	21.5	39.4
0	21.1	39.4
0	20.7	39.4
1	20.4	39.5
0	19.6	39.5
4	23.9	39.6
1	23.5	39.6
0	23.1	39.7
2	22.7	39.7
1	22.3	39.7
3	21.9	39.8
2	21.5	39.8
2	21.1	39.8
2	20.7	39.8
2	20.4	39.8
1	20.0	39.9
0	19.6	39.9
2	24.0	40.1
1	23.6	40.1
1	23.2	40.1
0	22.8	40.2
5	22.4	40.2
3	22.0	40.2
0	21.6	40.3
3	21.2	40.3
3	20.9	40.3
4	20.5	40.4
1	20.2	40.4
2	19.9	40.4
2	24.0	40.6
2	23.6	40.6
0	23.3	40.6
1	22.9	40.7
1	22.5	40.7
0	22.1	40.7
2	21.7	40.7
1	21.3	40.7
3	20.9	40.8
1	20.6	40.8
3	20.3	40.8
0	20.0	40.9
0	19.6	40.9
1	24.0	41.0
0	23.6	41.0
1	23.3	41.0
1	22.9	41.1
1	22.5	41.1
1	22.1	41.1
0	21.7	41.1
2	21.3	41.2

APPENDIX IV (Continued)

Crater density data for Mare Humorum.

No. of Craters	Lat.	Long.
3	20.9	41.2
1	20.6	41.2
1	20.3	41.2
2	20.0	41.3
0	19.6	41.3
0	24.0	41.4
3	23.6	41.4
0	23.3	41.4
0	22.9	41.5
2	22.5	41.5
0	22.1	41.5
1	21.7	41.5
2	21.3	41.5
0	20.9	41.6
1	20.6	41.6
2	20.3	41.6
1	20.0	41.6
2	19.6	41.7
2	19.3	41.7
0	24.0	41.8
3	23.6	41.8
3	23.3	41.8
2	22.9	41.9
2	22.5	41.9
2	22.1	41.9
0	21.7	41.9
1	21.3	42.0
2	20.9	42.0
3	20.6	42.0
3	20.3	42.0
1	20.0	42.1
2	19.6	42.1
0	19.3	42.1
2	24.0	42.3
1	23.6	42.3
1	23.3	42.3
0	22.9	42.3
3	22.5	42.3
2	22.1	42.4
0	21.7	42.4
2	21.3	42.4
1	20.9	42.4
3	20.6	42.4
1	20.3	42.5
2	20.0	42.5
3	19.6	42.5
3	19.3	42.5
1	24.0	42.7
1	23.6	42.7
0	23.3	42.7
1	22.9	42.7
0	22.5	42.8
3	22.1	42.8
1	21.7	42.8
0	21.3	42.8
1	20.9	42.8
0	20.6	42.9
4	20.3	42.9
1	20.0	42.9
4	19.6	42.9
4	24.0	43.1
2	23.6	43.1
1	23.3	43.1
2	22.9	43.2
1	22.5	43.2
2	22.1	43.2
2	21.7	43.2
3	21.3	43.3
3	20.9	43.3
2	20.5	43.3
2	24.0	43.6
1	23.6	43.7
2	25.6	32.3
0	25.2	32.3
1	24.7	32.4
3	24.2	32.4
2	23.8	32.5
3	25.9	32.7
2	25.6	32.7
1	25.2	32.8
0	24.7	32.8
0	24.3	32.9
2	23.8	33.0
3	25.9	33.1
0	25.6	33.1
1	25.2	33.2
0	24.7	33.3
1	24.3	33.3
0	23.9	33.4
2	26.0	33.5
3	25.6	33.6
1	25.2	33.6
2	24.7	33.7
1	24.3	33.7
0	24.0	33.8
4	26.0	33.9
2	25.6	34.0
1	25.2	34.0
0	24.8	34.0
1	24.4	34.1
2	24.0	34.3
1	26.0	34.3

APPENDIX IV (Continued)

Crater density data for Mare Humorum.

No. of Craters	Lat.	Long.	No. of Craters	Lat.	Long.
2	25.6	34.4	2	28.0	35.5
3	25.2	34.4	2	27.7	35.6
0	24.8	34.5	3	27.3	35.7
0	24.4	34.5	3	26.9	35.7
0	24.1	34.6	2	26.5	35.7
1	23.3	43.7	0	29.5	35.8
2	22.9	43.7	2	28.8	35.9
2	22.5	43.7	2	28.5	35.9
0	22.1	43.8	0	28.1	36.0
1	21.7	43.8	1	27.8	36.0
0	24.0	44.1	4	27.4	36.0
4	23.6	44.1	3	26.9	36.1
1	23.3	44.2	0	26.5	36.2
2	22.9	44.2	1	28.9	36.4
1	22.5	44.2	1	28.5	36.4
2	22.2	44.3	1	28.1	36.4
2	24.0	44.6	1	27.8	36.5
3	23.6	44.6	0	27.4	36.5
1	23.3	44.6	2	27.0	36.5
0	23.0	44.7	1	26.6	36.5
0	22.6	44.7	3	29.3	36.7
2	24.0	45.0	0	28.9	36.8
1	23.6	45.0	2	28.5	36.8
3	23.3	45.1	1	28.1	36.9
0	23.0	45.1	3	26.5	45.2
2	24.0	45.5	1	26.0	45.2
3	23.6	45.5	4	25.6	45.3
1	26.1	31.8	1	25.2	45.3
5	26.1	31.6	1	24.8	45.3
3	25.5	31.7	3	24.4	45.4
2	25.1	31.7	1	26.2	31.8
0	24.6	31.7	3	26.7	32.1
0	24.2	31.8	4	26.3	32.2
1	25.8	31.9	1	27.1	32.4
3	25.5	32.0	1	26.7	32.5
2	25.1	32.0	2	26.3	32.5
1	24.6	32.1	1	26.3	32.9
0	24.2	32.1	1	27.8	33.3
2	23.8	32.2	0	28.2	33.7
0	25.9	32.3	0	27.8	33.8
1	28.8	34.9	1	26.8	33.9
1	28.4	35.0	2	26.4	33.9
1	28.0	35.0	1	28.6	34.0
0	27.6	35.1	1	28.3	34.0
1	27.2	35.1	3	27.9	34.1
3	26.8	35.2	1	27.5	34.1
3	26.5	35.2	3	27.2	34.1
1	29.5	35.3	1	26.8	34.2
0	29.2	35.3	4	26.4	34.2
0	28.8	35.4	1	28.6	34.4
2	28.4	35.5	2	27.9	34.5

APPENDIX IV (Continued)

Crater density data for Mare Humorum.

No. of Craters	Lat.	Long.	No. of Craters	Lat.	Long.
0	27.5	34.5	3	26.6	37.4
4	27.2	34.6	2	29.0	37.6
2	26.8	34.6	1	28.6	37.7
3	26.4	34.7	2	28.2	37.7
0	29.2	34.9	2	28.2	34.5
0	27.9	40.1	3	27.8	37.8
1	27.6	40.2	0	27.5	37.8
0	27.3	40.2	3	27.1	37.8
2	26.8	40.3	2	26.7	38.0
0	27.9	40.6	0	28.6	38.2
1	27.6	40.6	1	28.2	38.2
3	27.2	40.6	2	27.8	38.3
2	26.7	40.7	2	27.5	38.3
0	27.9	41.0	0	27.1	38.3
1	27.5	41.1	0	26.7	38.4
4	27.1	41.1	2	27.9	38.8
2	26.7	41.2	3	27.5	38.8
3	27.5	41.5	3	26.7	38.8
0	27.2	41.5	1	27.2	39.2
1	26.7	41.5	0	26.7	39.3
2	26.7	42.0	0	27.8	39.7
2	27.2	42.4	0	27.5	39.7
0	26.7	42.5	0	27.2	39.8
2	27.2	42.8	2	26.8	39.8
4	26.8	42.9	0	26.0	42.6
3	27.6	43.3	1	25.6	42.6
2	27.2	43.4	3	25.2	42.6
0	26.7	43.4	1	24.7	42.7
2	27.6	43.8	3	24.3	42.7
6	27.3	43.8	3	26.4	43.0
0	26.7	43.9	1	26.0	43.0
1	27.9	44.1	0	25.6	43.0
2	27.6	44.2	1	25.2	43.1
3	27.3	44.3	0	24.7	43.1
3	26.7	44.3	3	24.3	43.2
1	27.6	44.6	2	26.4	43.5
3	27.4	44.6	3	26.0	43.6
0	26.8	44.7	1	25.7	43.7
0	27.4	45.0	1	25.3	43.7
1	26.8	45.0	1	24.8	43.8
0	27.8	36.9	0	24.4	43.8
3	27.4	36.9	2	26.4	43.9
0	27.0	37.0	1	26.0	44.0
1	26.6	37.0	1	25.7	44.0
0	29.3	37.2	1	23.5	44.1
0	28.9	37.2	2	24.8	44.1
0	28.5	37.2	0	24.4	44.2
0	28.1	37.3	0	26.4	44.4
2	27.8	37.3	0	26.0	44.4
1	27.5	37.3	2	25.7	44.4
0	27.1	37.4	1	25.3	44.5

Crater density data for Mare Humorum.

No. of Craters	Lat.	Long.
1	24.8	44.5
1	24.4	44.6
1	26.4	44.8
3	26.0	44.9
1	25.7	44.9
5	25.3	45.0
2	24.8	45.0
4	24.4	45.1
1	25.5	39.9
1	25.1	39.9
3	24.7	40.0
0	24.3	40.0
1	26.3	40.2
3	26.0	40.2
4	25.6	40.3
0	25.2	40.3
1	26.0	40.6
2	25.6	40.7
1	25.2	40.7
2	24.7	40.7
3	24.3	40.8
2	26.3	41.1
3	26.0	41.2
2	25.6	41.2
0	25.2	41.3
3	24.7	41.3
3	24.3	41.4
6	26.3	41.6
1	26.0	41.6
1	25.6	41.7
2	25.2	41.7
0	24.7	41.8
1	24.3	41.8
2	26.0	42.1
3	25.6	42.1
1	25.2	42.2
4	24.7	42.2
0	24.3	42.3
0	26.4	42.5
1	25.0	37.2
0	24.6	37.3
1	24.2	37.3
1	26.2	37.5
1	25.8	37.5
3	25.4	37.6
3	24.3	40.4
0	26.3	40.6
0	25.0	37.6
3	24.6	37.7
0	24.2	37.7
0	26.3	37.9
3	25.9	38.0
3	25.4	38.0
5	25.0	38.1
0	24.6	38.1
1	24.2	38.2
1	26.3	38.5
0	25.9	38.5
0	25.4	38.6
2	25.0	38.6
3	24.6	38.7
0	24.2	38.7
2	26.3	38.8
2	25.9	38.8
1	25.4	38.9
2	25.0	38.9
1	24.6	39.0
0	24.2	39.0
1	26.3	39.3
1	25.9	39.4
1	25.4	39.4
1	25.0	39.4
1	24.6	39.5
0	24.2	39.5
1	26.3	39.8
1	25.9	39.9
1	26.0	34.8
1	25.6	34.9
1	25.2	34.9
2	24.4	35.0
2	24.1	35.1
0	26.1	35.3
3	25.7	35.3
1	25.3	35.4
2	24.9	35.4
2	24.6	35.5
0	24.2	35.5
0	26.1	35.7
2	25.7	35.7
4	25.3	35.7
3	24.9	35.8
1	24.6	35.8
0	24.2	35.9
2	26.2	36.0
2	25.8	36.1
0	25.4	36.1
1	25.0	36.1
1	24.6	36.2
3	24.2	36.2
3	26.2	36.4
1	25.8	36.5
1	25.4	36.5

APPENDIX IV (Continued)

Crater density data for Mare Humorum.

No. of Craters	Lat.	Long.	No. of Craters	Lat.	Long.
1	25.0	36.6			
0	24.6	36.7			
1	24.2	36.7			
0	26.2	37.0			
1	25.8	37.0			
1	25.4	37.1			
1	23.5	32.5			
2	23.5	32.7			
0	23.1	32.7			
0	22.7	32.8			
1	22.3	32.9			
1	21.9	33.0			
3	23.5	33.1			
2	23.1	33.2			
0	22.7	33.3			
0	22.3	33.3			
0	21.9	33.4			
2	21.5	33.5			
0	23.6	33.5			
1	23.3	33.6			
0	22.9	33.6			
0	22.5	33.7			
0	22.0	33.7			
0	21.5	33.8			
0	21.0	33.8			
2	20.6	33.9			
3	20.2	33.9			
0	19.8	33.9			
1	23.6	42.1			
4	21.7	38.8			
1	28.4	35.0			
1	23.6	33.9			
0	23.2	33.9			
0	22.8	34.0			
0	22.4	34.0			
1	22.0	34.1			
1	20.0	39.5			
1	19.9	35.9			
4	19.9	37.2			
0	22.7	39.3			
5	26.1	31.5			